Bollettino di Geofisica Teorica ed Applicata Vol. 56, n. 2, pp. 295-328; June 2015
DOI 10.4430/bgta0141

The contribution of pattern recognition of seismic and morphostructural data to seismic hazard assessment

A. Peresan[1,3,5*], A. Gorshkov[1,2], A. Soloviev[1,2] and G.F. Panza[1,3,4,5]

[1] *The Abdus Salam International Centre for Theoretical Physics, SAND Group, Trieste, Italy*
[2] *IEPT of Russian Academy of Sciences, FASO, Moscow, Russian Federation*
[3] *Department of Mathematics and Geosciences, University of Trieste, Italy*
[4] *Institute of Geophysics, China Earthquake Administration, Beijing, China*
[5] *International Seismic Safety Organization (ISSO), Arsita, Italy*

(Received: April 19, 2014; accepted: December 22, 2014)

ABSTRACT Experience from the destructive earthquakes worldwide, which occurred over the last decade, motivated an active debate discussing the practical and theoretical limits of the seismic hazard maps based on a classical probabilistic seismic hazard approach (PSHA). Systematic comparison of the observed ground shaking with the expected one, in fact, shows that such events keep occurring where PSHA predicted seismic hazard to be low. Amongst the most debated issues is the reliable statistical characterization of the spatial and temporal properties of large earthquakes occurrence, due to the unavoidably limited observations from past events. We show that pattern recognition techniques allow addressing these issues in a formal and testable way and thus, when combined with physically sound methods for ground shaking computation, like the neo-deterministic approach (NDSHA), may produce effectively preventive seismic hazard maps. Pattern recognition analysis of morphostructural data provide quantitative and systematic criteria for identifying the areas prone to the largest events, taking into account a wide set of possible geophysical and geological data, whilst the formal identification of precursory seismicity patterns (by means of CN and M8S algorithms), duly validated by prospective testing, provides useful constraints about impending strong earthquakes at the intermediate space-time scale. According to a multi-scale approach, the information about the areas where a strong earthquake is likely to occur can be effectively integrated with different observations (e.g., geodetic and satellite data), including regional scale modelling of the stress field variations and of the seismic ground shaking, so as to identify a set of priority areas for detailed investigations of short-term precursors at local scale and for microzonation studies. Results from the pattern recognition of earthquake prone areas ($M \geq 5.0$) in the Po Plain (northern Italy), as well as from prospective testing and validation of the time-dependent NDSHA scenarios are presented, including the case of the May 20, 2012 Emilia earthquake.

Key words: precursory seismicity patterns, earthquake prone areas, morphostructural analysis, neo-deterministic seismic hazard.

* presently at Ist. Naz. Oceanografia e Geofisica Sperimentale, Udine, Italy

1. Introduction

Over the last decade, the large and most destructive earthquakes worldwide kept occurring in areas where the seismic hazard predicted by classical maps based on probabilistic seismic hazard analysis (PSHA) (Giardini *et al.*, 1999) was comparatively lower (Geller, 2011; Stein *et al.*, 2012; Wyss *et al.*, 2012). The unsatisfactory anticipatory capability of PSHA maps motivated an active debate discussing their practical and theoretical limits (e.g., Peresan *et al.*, 2012; Gulkan, 2013; Stein *et al.*, 2013 and references therein). Amongst the raised questions, several point to the limits in the reliable characterization of the spatial and temporal properties of potential earthquake sources, namely:

- is the available information about past seismicity sufficient to constrain the areas where large earthquakes may occur?
- does the available information about past seismicity allow us to constrain the statistical models and to provide reliable estimates of their probability of occurrence within narrow regions?

Recent destructive earthquakes suggest this might not be the case; most of them, indeed, occurred in areas where other relevant events were not reported before. This observation is particularly critical when dealing with the classical probabilistic (PSHA) approach to seismic hazard assessment, which requires the definition of earthquake probability models within narrow seismic sources, often resorting to simplistic and untestable assumptions, poorly constrained by available observations (e.g., Poissonian earthquakes occurrence, characteristic earthquake model, etc.).

The heuristic limitations are, indeed, a major limit of PSHA: the available short earthquake catalogues worldwide do not allow the statistics inference theory to project the present time probabilistic estimation over periods of time as long as 1000-10000 years. Clearly, the map tries to predict events, which do not have a significant statistics within the input data, and most probably many of them did not even appear yet, accordingly with the characteristic time of geological process leading to seismogenesis. This calls for the integration of the information provided by earthquake catalogues with additional geological and geophysical pieces of evidence, independent from observed seismicity. However, with PSHA it is quite difficult, if not impossible, to take in due account the information given by paleoseismicity (e.g., Michetti *et al.*, 2012), morphostructural analysis (Gorshkov *et al.*, 2003) or similar studies (e.g., Brune and Whitney, 2000). In fact, though geological and geophysical evidence may contribute to identify areas where large, yet unobserved earthquakes may occur, defining the associated probability distribution is by far a much more difficult problem, particularly in view of the large uncertainties and incompleteness characterizing such information.

We show in this paper that pattern recognition techniques allow us addressing the above questions in a formal and testable way and thus, when combined with physically sound methods for ground shaking computation, like the neo-deterministic approach [NDSHA: Panza *et al.* (2012)], may significantly contribute to the definition of effectively preventive seismic hazard maps.

The first application of pattern recognition to the identification of potential locations of strong earthquakes has been introduced in the 1970s by Gelfand *et al.* (1972). The approach is based on the assumption that large earthquakes are correlated with the nodes formed around lineaments intersections. The nodes are delineated by morphostructural zoning (MZ) method that is based on geomorphic and geological data and does not use the knowledge about past seismicity (Alekseevskaya *et al.*, 1977). The pattern recognition technique is employed to select

among all the nodes those, which are prone to earthquakes above a certain (target) magnitude. Since the early 1970s the methodology has been successfully applied in a number of regions worldwide, including California, where it permitted the identification of earthquake prone areas that have been subsequently struck by strong events and that previously were not considered seismogenic [see the overviews by Gorshkov *et al*. (2003) and Soloviev *et al*. (2014)]. The reliability and statistical significance of the methodology is supported by the number of strong earthquakes that occurred in the previously studied regions: 87% of the post-publication events with relevant magnitudes occurred within the nodes that were recognized in advance as capable of target earthquakes (Soloviev *et al*., 2014).

The morphostructural analysis has been already applied to the Italian mountain ranges, namely in the Alps (Gorshkov *et al*., 2004) and in peninsular Italy and Sicily (Gorshkov *et al*., 2002). In this study the analysis is applied for the identification of earthquake prone areas ($M \geq 5.0$) in the Po Plain (northern Italy), following the specific formal criteria of MZ recently defined for plain areas, where special attention is paid to drainage pattern (variant MZ_P). The feasibility of such analysis (MZ_P) has been established for topographically flat basins within Iberian Peninsula (Gorshkov *et al*., 2010) and recently for the Rhone Valley in France (Gorshkov and Gaudemer, 2012). In 2012 the south-eastern part of the Po Plain, Emilia Romagna region, was struck by an M=6.1 earthquake, which occurred within one of the nodes delineated by MZ_P; we show that, if the recognition would have been performed any time before the event after the formalization of MZ_P the node hosting the May 20, 2012 Emilia Romagna earthquake could have been properly recognized as prone to $M \geq 5.0$ earthquakes.

A formal identification of priority areas, most prone to future seismic activation, can be performed integrating the space information provided by the earthquake prone areas with the space-time information provided by formally defined earthquakes predictions (e.g., Peresan *et al*., 2011). A number of forecasting methodologies have been developed, mainly based on the analysis of seismicity, and are currently applied both at national and international scale (Jordan *et al*., 2011). However, only few of them, including CN and M8S algorithms (Peresan *et al*., 2005), are defined in testable way and are undergoing rigorous prospective testing over a time span sufficient to validate, in a statistically reliable way, the obtained results. The algorithms make use of the information provided by standard earthquake catalogues to identify the periods of time when a strong earthquake (with magnitude above a predefined threshold) is likely to occur within a region with linear dimensions of few hundred kilometres. CN and M8S, which are based on the diagnosis of formally defined premonitory seismicity patterns, have demonstrated effective and statistically significant results in rigorous real-time testing, ongoing for more than a decade over the Italian territory (Peresan *et al*., 2011) and about two decades on a global scale (Kossobokov, 2012).

The indications provided by pattern recognition procedures can be used to focus the investigation of possible local scale precursors in the areas (with linear dimensions of few tens kilometres), where the probability of a strong earthquake is relatively high, as well as for drawing time-dependent scenarios of ground shaking by the NDSHA approach (Peresan *et al*., 2011). Accordingly, a set of deterministic scenarios of ground motion at bedrock, which refers to the time interval when a strong event is likely to occur within the alerted area, can be defined by means of full waveform modelling, both at regional and local scale.

In Italy CN and M8S predictions, as well as the related time-dependent ground motion

scenarios associated with the alarmed areas, are routinely updated every two months since 2006. The prospective application of the time-dependent NDSHA approach allows for a rigorous testing and validation of the proposed methodology and, at the same time, provides information that can be useful in assigning priorities for timely mitigation actions. As an example, in the areas where ground shaking values greater than 0.2 g are estimated at bedrock, further investigations can be performed taking into account the local soil conditions, to assess the performances of relevant structures, such as historical and strategic buildings.

2. State of art in pattern recognition of earthquake prone areas

A systematic and testable assessment, capable of providing first-order consistent information about the sites where large earthquakes may occur, is highly important for knowledgeable seismic hazard evaluation. One of the approaches to the solution of this problem was introduced in the early 1970s by Gelfand *et al*. (1972). The approach is based on the hypothesis that the strong earthquakes nucleate at the morphostructural "nodes", namely the intersections of morphostructural lineaments. Here the term "lineament", as will be described in section 2.1., is used with a quite different meaning with respect the early one introduced by Hobbs (1904). Within the study region an earthquake is defined as "strong" if its magnitude $M \geq M_0$, where M_0 is a threshold specified depending on the seismicity level of the region. The nodes are delineated by the specific MZ method (Alekseevskaya *et al*., 1977; Rantsman, 1979; Gorshkov *et al*., 2003). The hypothesis that the epicentres of the strong earthquakes correlate with the lineaments intersections is supported by the statistical analysis of their locations, proposed by Gvishiani and Soloviev (1981). The few exceptions to this hypothesis can be explained by the possible errors in both determining the location and size of the earthquakes and in the mapping of the morphostructural nodes.

Since the systematic instrumental seismological observations dates back only about 100 years and the available earthquake catalogues cover a time span rather short compared to characteristic time of tectonic processes, it is reasonable to assume that not all the potentially seismogenic nodes are marked by strong earthquakes during the period covered by instrumental and macroseismic observations. For a partial but effective solution of this problem, Gelfand *et al*. (1972) proposed to apply pattern recognition methods, specifically the Cora-3 algorithm with learning designed by Bongard (1967). The nodes are treated as the objects of recognition; each object is associated with the vector of topographic, geological and geophysical parameters describing nodes. The sample nodes needed for training the pattern recognition algorithm are selected taking into account the data about seismicity recorded in the region. The output of the recognition includes: 1) the classification of the nodes into those prone to earthquakes with $M \geq M_0$ and those, where only the events with $M < M_0$ are possible, and 2) the criteria (the decision rule) governing the classification. The criteria are based on topographic, geological, and geophysical parameters characterizing the nodes.

2.1. Pattern recognition applied to earthquake prone areas identification

The recognition of earthquake prone areas includes the following steps:

- outline of the region and specification of the magnitude M_0 which defines the "strong"

earthquake for a given region;
- morphostructural zonation of the region and specification of the objects of recognition;
- selection of the sample sets used for the training of the pattern recognition algorithm;
- selection of the parameters for the description of the objects of recognition and measurement of their values;
- discretization of the values of the parameters and their conversion into binary vectors;
- application of a pattern recognition algorithm in order to classify the objects of recognition into two classes: the seismogenic objects prone to $M \geq M_0$ and non-seismogenic ones with respect to M_0;
- estimation of the reliability of the classification by control tests.

When selecting the region for the study, two main factors are taken into account. Firstly, the region should be relatively homogeneous with respect to the tectonic regime governing the seismogenesis in the region. Secondly, the number of recorded events with target magnitude should be sufficient to form the representative sample set for the training of the pattern recognition algorithms. Once the region is specified, the MZ is carried out to delineate the morphostructural nodes, which are then treated as recognition objects.

Since 1972 the methodology has been applied for the recognition of earthquake prone areas for different M_0 in many seismic regions of the world, specifically, in the Tien Shan and Pamir (Gelfand *et al*., 1972), united region of Balkans, Asia Minor, Transcaucasia (Gelfand, 1974a, 1974b), California and Nevada (Gelfand *et al*., 1976), Italy (Caputo *et al*., 1980; Gorshkov *et al*., 2002), Andean South America (Gvishiani and Soloviev, 1984), Kamchatka (Gvishiani *et al*., 1984), western Alps (Cisternas *et al*., 1985), Pyrenees (Gvishiani *et al*., 1987), Greater Caucasus (Gvishiani *et al*., 1988), Lesser Caucasus (Gorshkov *et al*., 1991), Himalaya (Bhatia *et al*., 1992), Carpathians (Gorshkov *et al*., 2000), Alps and Dinarides (Gorshkov *et al*., 2004), Alborz (Gorshkov *et al*., 2009a), Ecuador (Chunga *et al*., 2010), Iberian Plate (Gorshkov *et al*., 2010), North Vietnam (Tuyen *et al*., 2012), Kopet Dagh (Novikova and Gorshkov, 2013), Caucasus region (Soloviev *et al*., 2013). The other applications of pattern recognition techniques for seismic hazard analysis were recently reviewed by Mridula *et al*. (2013).

2.1.1. Morphostructural zoning method

In the MZ (Alekseevskaya *et al*., 1977; Gorshkov *et al*., 2003), the study region is divided into a system of hierarchically ordered areas, characterized by homogeneous present-day topography and tectonic structure. MZ distinguishes: 1) blocks (areas) of different rank; 2) their boundary zones, morphostructural lineaments; and 3) sites where lineaments intersect, the nodes. A morphostructural lineament is viewed as a boundary zone between territorial units delineated by MZ. The rank of the lineament depends on the rank of the area limited by the lineament. With respect to the regional trend of the tectonic structure and topography, two types of lineaments are distinguished: 1) longitudinal and 2) transverse ones. Longitudinal lineaments are approximately parallel to the regional strike of the tectonic structure and of the topography and, as a rule, include the prominent faults. Transverse lineaments go across the regional trend of the tectonic structure and of the topography. Normally, they appear on the Earth's surface discontinuously and are evidenced by escarpments, by rectilinear parts of river valleys, and partly by faults.

The MZ method differs from the standard morphostructural analysis where the term "lineament" (Hobbs, 1904) is used to define the complex of alignments detectable on

topographic maps or on satellite images. According to that definition, the lineament is locally defined and the existence of the lineament does not depend on the features of the surrounding areas. In MZ, the primary element is the block - a relatively homogeneous area - while the lineament is a secondary element of the morphostructure. The boundaries of the blocks correspond to the lineaments; this means that the existence and the position of the lineaments are determined not locally, but as a part of a broader hierarchical structure. If a certain alignment does not separate two topographically different areas, that alignment cannot be viewed as a lineament in MZ; therefore, the lineaments are secondary features with respect to the blocks.

Since MZ is based mainly on topographic data, the method is applicable for studying practically any areas of the Earth including sea and oceanic floors if topographic and/or bathymetric data are available for the study region. The only exceptions are the desert areas where mobile Aeolian landforms prevail. The first attempt to study the sea floor with MZ has been made by Novikova *et al.* (2012) for the deep south Caspian basin. The MZ map of the basin has been used for recognizing seismogenic nodes prone to M6+.

Morphostructural nodes are formed around the intersections or junctions of two or more lineaments. A node may include more than one intersection or junction. Nodes are characterized by a mosaic combination of various topographic forms and by an increased number of linear topographic forms of various strikes that reveal the instability of the area.

The methodology treats the nodes as earthquake-controlling structures. Nodes are the areal structures, boundaries of which can be delineated through long-term field work, as it has been proven in central Asia and the Greater Caucasus (Rantsman, 1979; Gvishiani *et al.*, 1988). However, the delineation of the boundaries of the nodes is a cumbersome task and it requires large-scale MZ of lineament intersection areas based on field studies. An attempt to delineate structurally bounded nodes has been made by Gorshkov *et al.* (2009b) in the Alps-Dinarides junction zone on the base of the analysis of large-scale topographic and geological maps. But in most of the previously studied regions the intersections of morphostructural lineaments were treated as recognition patterns. In such case, the nodes are defined as the circles of a certain radius, which depends on the target M_0 in accordance with the empirical relation between magnitude and the earthquake source (Wells and Coppersmith, 1994).

The fact that earthquakes are nucleated within the nodes was first established from the field geomorphic observations in central Asia by Gelfand *et al.* (1972) and then it was proved in all other regions studied with this methodology (Gelfand *et al.*, 1974a, 1974b, 1976; Caputo *et al.*, 1980; Gvishiani and Soloviev, 1984; Gvishiani *et al.*, 1984, 1987, 1988; Cisternas *et al.*, 1985; Gorshkov *et al.*, 1991, 2000, 2002, 2004, 2009a, 2010; Bhatia *et al.*, 1992; Chunga *et al.*, 2010; Tuyen *et al.*, 2012; Novikova *et al.*, 2013; Soloviev *et al.*, 2013).

The correlation of earthquakes with fault zone intersections in different tectonic environments was also evidenced by Talwani (1988), Hudnut *et al.* (1989), Girdler and McConnell (1994). The model proposed by Talwani (1999) demonstrates that intersecting fault zones provide a location for stress accumulation. According to King (1986), fault zones intersections provide locations for the initiation and healing of ruptures. A model proposed by Gabrielov *et al.* (1996) implies that block interaction along intersecting lineaments leads to stress and strain accumulation and secondary faulting around the intersection. This causes the generation of new faults and blocks of progressively smaller size, so that a hierarchical mosaic structure, essentially a node, is formed around the intersection.

2.1.2. Recognition of earthquake prone areas

Since strong earthquakes are spatially correlated with nodes possessing some specific features, the identification of earthquake prone areas can be formulated as a pattern recognition problem, where the nodes are the objects of recognition. Specifically, the pattern recognition algorithm is applied in order to classify the nodes into two classes: D ("dangerous") nodes, which can host earthquakes with $M \geq M_0$, and the nodes N ("not dangerous") where earthquakes with $M \geq M_0$ cannot occur.

The application of recognition algorithms with learning requires the preliminary selection of a training sample set W_0. This set consists of two non-overlapping subsets of objects with known classification, namely: the D_0 objects that are examples of class D, and the N_0 objects that are examples of class N. In this specific application the sample $W_0=D_0 \cup N_0$ is constructed in the following way. The subset D_0 is composed of nodes that are already marked by earthquakes with $M \geq M_0$. The subset N_0 is either composed by the remaining nodes of W, $N_0=W \backslash D_0$, or by the nodes where smaller events, with $M \geq M_0-\delta$ (δ is typically about 0.5), are unknown. We note that it is practically impossible to select an "uncontaminated" training set N_0 for class N, since it is impossible to guarantee *a priori* that a node assigned to N_0 is certainly an aseismic one.

Each node is associated with a vector. The recognition algorithms are applied to the vectors, whose components are given by the values of the parameters describing the nodes. Parameters of the nodes should characterize some properties of the node environments that reflect the different factors relevant to seismicity. During the studies on recognition of earthquake prone areas (Gelfand *et al*., 1972, 1974a, 1974b, 1976; Caputo *et al*., 1980; Gvishiani and Soloviev, 1984; Cisternas *et al*., 1985; Gvishiani *et al*., 1988; Gorshkov *et al*., 1991, 2000, 2002, 2003, 2004, 2009a, 2010; Bhatia *et al*., 1992) different parameters describing the nodes have been tested. These parameters include the geomorphic and morphometric information, the characteristics of the block-and-lineament geometry, and the gravity data. In principle, any information characterizing the specific features of seismic areas can be used for recognition. The only necessary precondition is that the value of each parameter should be defined with the same accuracy for all the objects (i.e., the nodes) within the studied territory.

Once the values of the parameters have been specified, all the objects contained in W are converted into the vectors $\mathbf{w}i = \{w_1^i, w_2^i, ..., w_m^i,\}$, $i = 1, 2, ..., n$, where m is the total number of the parameters; n is the total number of the objects in the set W; w_k^i is the value of the kth parameters measured for the ith object. Normally, the Cora-3 recognition algorithm (Bongard, 1967) is used for the classification of nodes. The algorithm operates with binary vectors. Therefore, the initial values of the parameters should be converted into binary vectors. The conversion is carried out by the procedures of discretization and coding (Gelfand *et al*., 1976; Gvishiani *et al*., 1988; Gorshkov *et al*., 2003). After the conversion, the recognition algorithm carries out the classification of the objects using the training sample $W_0=(D_0, N_0)$: $\mathbf{W}=\mathbf{D} \cup \mathbf{N}$, where **D** and **N** are the vectors assigned by the algorithm to the classes D and N, respectively. In every detail the Cora-3 algorithms and some others used for recognition of earthquake prone areas are described in Gelfand *et al*. (1976) and Gorshkov *et al*. (2003).

The quality of the final classification defined by the recognition algorithm can be evaluated by the control tests. A number of such tests have been developed to estimate the stability of the final classification (Gelfand *et al*., 1976; Gvishiani *et al*., 1988; Gorshkov *et al*., 2003). The positive results of the control tests suggest that the objects of recognition are properly subdivided into the

D and N classes. Evidence about historical and paleo-earthquakes is also taken into account in the evaluation of the final classification of the nodes. Clearly, the final response about the reliability of the recognition results obtained for the studied region may only come by prospective testing, accounting for the subsequent target earthquakes occurred after the nodes classification.

2.2. Validation of the results of nodes recognition

During the last 40 years the recognition of earthquake prone areas has been performed for a number of seismically active regions (Gelfand *et al.*, 1972, 1974a, 1974b, 1976; Caputo *et al.*, 1980; Gvishiani and Soloviev, 1984; Gvishiani *et al.*, 1984, 1987, 1988; Cisternas *et al.*, 1985; Gorshkov *et al.*, 1991, 2000, 2002, 2004, 2009a, 2010; Bhatia *et al.*, 1992; Chunga *et al.*, 2010; Tuyen *et al.*, 2012; Novikova and Gorshkov, 2013; Soloviev *et al.*, 2013). Most of the regions have been struck by the post-publication earthquakes of target magnitudes. These events provide the necessary information to assess the reliability of the results. The verification of the recognition results using the post-publication earthquakes has been periodically performed (Gorshkov *et al.*, 2003, 2005). The last verification has been made by Soloviev *et al.* (2014) using the earthquake parametric data provided by the U.S. National Earthquake Information Center (NEIC) as of August 1, 2012. Table 1 summarizes the results updated to April 2014. The table includes only the regions which were struck by the post-publication target events, with magnitudes $M \geq M_0$. In Italy, where the nodes recognition has been revised and extended during the last decade (Gorshkov *et al.*, 2002, 2004), we refer to the early publication by Caputo *et al.* (1980). In fact the results, for earthquakes that occurred in peninsular Italy and Sicily after the publication of the papers, are the same in both Caputo *et al.* (1980) and Gorshkov *et al.* (2002), evidencing the stability of recognition, whereas no target earthquake did occur since 2004 in the Alpine region analyzed by Gorshkov *et al.* (2004).

Noticeably, Table 1 includes the most recent M=8.2 earthquake (according to NEIC determinations), which occurred in Chile on April 2, 2014; the epicentre of this earthquake is located within a node that was recognized as prone to $M \geq 7.75$ by Gvishiani and Soloviev (1984).

Table 1 - Summary results of testing the reliability of recognition of the earthquake prone areas.

Region and year of the publication of the results	M_0	Number of post-publication target earthquakes in the region			
		total number	in the D nodes (including in the D* nodes)	in the N nodes	outside the nodes
Tien Shan and Pamir, 1972	6.5	7	6 (1)	0	1
Balkans, Asia Minor, and Transcaucasia, 1974	6.5	27	25 (7)	1	1
California and Nevada, 1976	6.5	14	13 (4)	0	1
Italy, 1980	6.0	8	4 (1)	0	4
South American Andes, 1982	7.75	6	5 (3)	1	0
Kamchatka, 1984	7.75	1	1	0	0
Western Alps, 1985	5.0	6	5 (1)	1	0
Pyrenees, 1987	5.0	6	5 (1)	1	0
Greater Caucasus, 1988	5.0	13	13 (9)	0	0
Himalaya, 1992	6.5	4	3 (1)	0	1
Iberia, 2010	5.0	1	1	0	0
Total		93	81(28)	4	8

D* is number of nodes where the target earthquakes have not been known before the recognition.

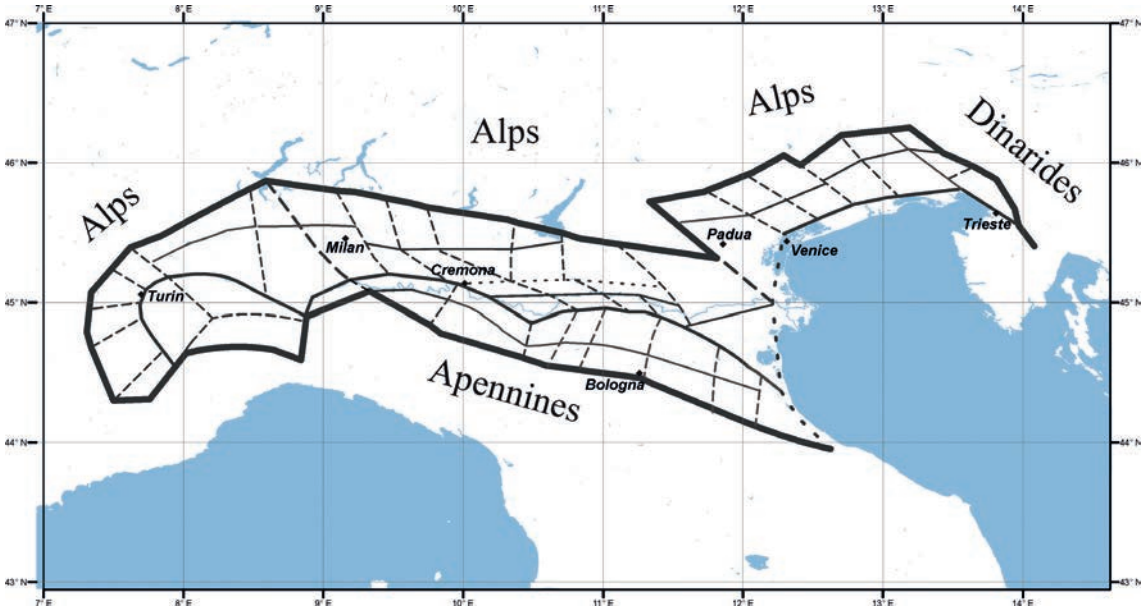

Fig. 1 - The MZ map of the Po Plain: lines outline morphostructural lineaments. Bold lines mark first rank lineaments, thick lines mark second rank lineaments, thin lines mark lineaments of third rank. Continuous lines correspond to longitudinal lineaments, while dashed lines indicate transverse lineaments.

Totally, 93 strong earthquakes have occurred in the regions listed in Table 1; specifically, 81 events (or 87%) fall in the seismogenic nodes D recognized in advance, and 28 out of these 81 earthquakes are located within the nodes D, where target events (earthquakes with $M \geq M_0$) were not yet observed at the moment of the recognition. Thus, the verification against independent data, i.e., the earthquakes that occurred after the publication of the maps, supports the reliability and statistical significance of the results of the recognition of the earthquake prone areas.

3. The morphostructural zonation and pattern recognition of earthquake prone areas in the Po Plain (northern Italy)

The recognition of earthquake prone areas was already carried out for the Italian mountain ranges, namely in the Alps (Gorshkov *et al*., 2004), peninsular Italy and Sicily (Gorshkov *et al*., 2002), using the pattern recognition approach. In this study, the analysis is extended to the flat areas in the Po Plain, to allow for the systematic identification of the nodes prone to earthquakes with magnitude $M \geq 5.0$.

3.1. Morphostructural zoning of the Po Plain

The preliminary MZ_P map of the Po Plain, shown in Fig. 1, has been compiled using topographical, tectonic and geological maps as well as satellite photos. Geophysical and geological data, available via the portal of the Italian Geological Service on ISPRA website (http://www.isprambiente.gov.it), as well as the DISS database of active faults (DISS Working Group, 2010), have been considered. Recent publications on geomorphology, tectonics,

seismotectonics and geophysical studies of the Po Plain have been taken into consideration as well (Castiglioni, 1999; Burrato *et al.*, 2003; Livio *et al.*, 2009; Toscani *et al.*, 2009; Handy *et al.*, 2010; Michetti *et al.*, 2012). The outlined map shows a hierarchical blocks-and-lineaments structure of the region and the locations of the morphostructural nodes which are formed around intersections or junctions of lineaments of different strike. This map has been used for the recognition of the nodes capable of earthquakes with $M \geq 5.0$, as described in the following.

The Po Plain is characterized by a flat topography. Our recent studies of topographically flat basins in the Iberian Peninsula (Gorshkov *et al.*, 2010) and the wider part of the Rhone Valley, between the western Alps and Massif Central (Gorshkov and Gaudemer, 2012), have demonstrated the applicability of MZ_P to the study of basins, with a relatively flat topography. The morphostructural analysis has been performed for the Po Plain, following to the specific formal criteria applied to plain areas where, besides topography, special attention is paid to drainage pattern.

A preliminary correlation analysis between the epicentres of past of earthquakes with $M \geq 5.0$ and the intersections of MZ_P lineaments has been performed. The information about earthquakes was selected from the Updated Catalog of Italy [UCI: Peresan and Panza (2002)], that covers the time span from year 1000 up to September 1, 2012. We found that the considered events well correlate with intersections of the morphostructural lineaments, namely the morphostructural nodes, thus allowing us to apply pattern recognition algorithms for the identification of nodes prone to earthquakes with $M \geq 5.0$ in the Po Plain.

3.2. Identification of earthquake-prone areas (M≥5.0) in the Po Plain by the pattern recognition technique

Following a procedure similar to that developed and applied in the Rhone Valley, France (Gorshkov and Gaudemer, 2012), a preliminary identification of the areas prone to earthquakes with magnitude larger or equal to 5.0 (referred as M5+ hereinafter) has been carried out for the Po Plain.

The nodes have been defined based on the map shown in Fig. 1. In total, 102 intersections of lineaments are identified and each intersection is treated as a node. Formally the node is defined as circle of radius R=20 km surrounding each point of intersection of lineaments. Such node dimension is consistent with the dimension of earthquake sources with $M \geq 5.0$ (Wells and Coppersmith, 1994).

The scope of the recognition analysis is to classify all the nodes, delineated within the study region, into one of the following two classes:

1. class D containing the nodes where earthquakes M5+ may occur (namely, the earthquake prone areas);
2. class N including the nodes where only smaller earthquakes may occur.

In this work, a two steps process, composed by a learning stage and a recognition stage is used to recognize the nodes prone to earthquakes with $M \geq 5.0$. At the learning stage, past earthquakes are taken into account to select the sample nodes of D and N classes for identifying the most informative parameters that discriminate D nodes from N nodes. In some cases, however, the learning stage is skipped, and the decision rules identified for other regions are directly used (e.g., Gorshkov et al., 2004). At the stage of recognition of the seismogenic nodes no use is made of the information about past seismicity, since the recognition is based only on morphological, geological and geophysical parameters of the nodes.

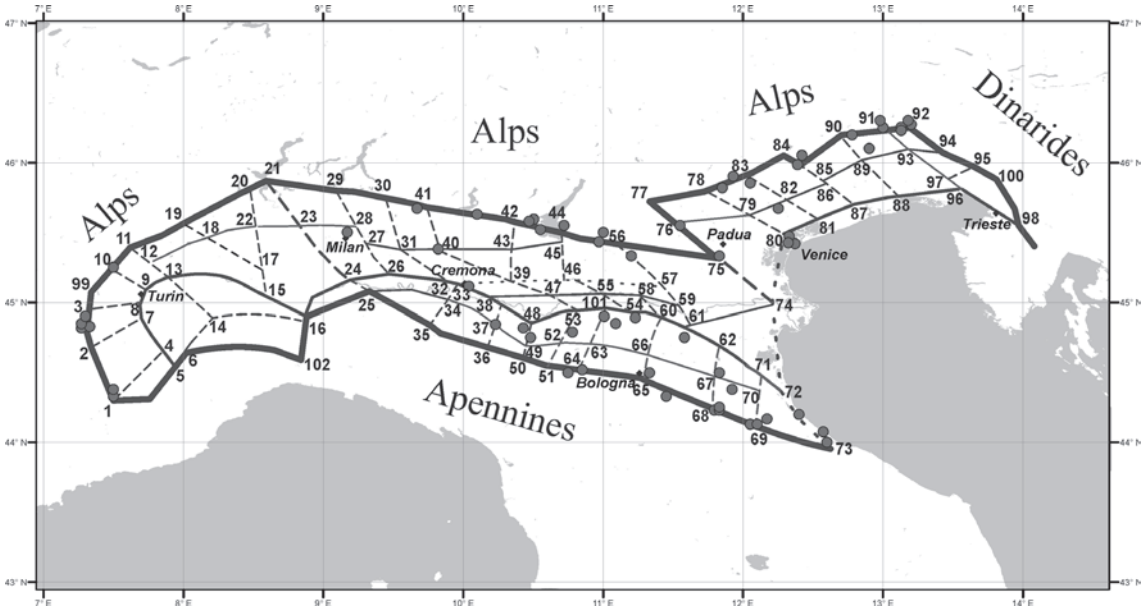

Fig. 2 - MZ map of the Po Plain and M5+ earthquakes occurred from 1093 to 2012. Lines depict lineaments of different rank (as in Fig. 1). Numbers identify the outlined nodes. Dots mark the epicentres of M5+ earthquakes from the UCI catalogue.

3.2.1. Seismicity data

To select the sample nodes for the learning stage, the information on the recorded events with $M \geq 5.0$ is taken into account, considering the UCI catalogue (Peresan and Panza, 2002). This earthquake catalogue covers the time span from 1000 year up to August 2012 and it is representative for events with $M \geq 5.0$ (M5+ earthquakes) from 1500 (Vorobieva and Panza, 1993; Panza *et al.*, 2010). The location and intensity of the selected earthquakes has been cross-checked with the information provided by the NT4.1 (Camassi e Stucchi, 1997) and CPTI11 (Rovida *et al.*, 2011) earthquake catalogues. Specifically, 71 earthquakes have been considered to select the nodes for the learning stage; 18 earthquakes are situated within the Po Plain, while 53 are located along the boundaries between the Po Plain and surrounding mountains. Their epicentres are mapped in Fig. 2 that shows how the considered earthquakes well correlate with intersections of morphostructural lineaments, which have been defined deliberately ignoring seismicity data. There is just one earthquake, occurred in 1894 (M=5.1), which cannot be associated with a specific node; its epicentre is located between nodes 41 and 42.

3.2.2. Definition of the parameters for the recognition process

In order to apply the pattern recognition algorithms, each node is described by a set of parameters, the list of which is provided in Table 2. The values of the parameters have been measured for each node using topographic, geological and gravity maps, as well as the MZ map shown in Fig. 1.

3.2.3. Recognition of nodes prone to earthquakes M5+

Out of the 102 nodes identified within the study region, 60 are located in lowland environments within the Po Plain and the remaining 42 sit on the first rank lineaments that

divide the Po Plain from the surrounding mountain chains. The considered parameters (Table 2), particularly the morphometric ones, differ significantly for the nodes located within the Po Plain and for the nodes related with the first rank lineaments that delimit the plain. Therefore the recognition has been performed separately for these two groups of nodes, applying the Cora-3 recognition algorithm to each of them.

Accordingly, at the learning stage all the nodes have been a priori divided into two sets, so as to define the training sets for the Cora-3 algorithm. Specifically, to assemble the set $\mathbf{D}_0$, the nodes situated most closely to the epicentres of past M5+ earthquakes are considered; the remaining nodes have been assigned to the set N_0.

Recognition of nodes located within the Po Plain. For the group of nodes located in the Po Plain, four variants of classification of nodes into classes D and N have been performed, in order to identify the most stable one. The results of recognition are summarized in Table 3. Three variants of recognition (I-III) have been obtained using a different learning set D_0. In the variant I, the set D_0 is formed using the nodes located most closely to the epicentres of all earthquakes shown in Fig. 1. In the variant II, the nodes 28 and 80 (Fig. 2), hosting only ancient earthquakes whose location is poorly defined, are excluded from D_0. Because the catalogue UCI is representative for M5+ since 1500, in the variant III we exclude from D_0 all the nodes hosting only events occurred before 1500 (specifically nodes 28, 33, 37, 80, 82, and 89). An additional classification of the nodes (IV) is obtained using the characteristic traits defined by Cora-3 for D and N nodes located in lowland areas of Iberia (Gorshkov *et al.*, 2010). A last, additional experiment is carried out excluding from D_0 the two nodes hosting the epicentres of the two earthquakes, which struck the Emilia Romagna region in May 2012 (i.e., nodes 54 and 101). Although the score of this last experiment is slightly less than those of variants I, II and III, both nodes are correctly recognized as D nodes.

Table 2 - Parameters used for recognition of seismogenic nodes in the Po Plain and corresponding thresholds for their discretization.

Parameters	Thresholds of discretization	
	Po Plain interiors	Po Plain boundaries
A) Topographic parameters		
Maximum topographic altitude, m (Hmax)	30 20	901 1600
Minimum topographic altitude, m (Hmin)	5 30	70 180
Relief energy, m (ΔH) (Hmax - Hmin)	27 200	906 1560
Distance between the points Hmax and Hmin, km (L)	27 34	2 34
Slope, (ΔH/L)	2.1	32.2 61.8
B) Geological parameters		
The portion of the node area covered by soft (quaternary) sediments, %, (Q)	70 98	15 25
C) Parameters from the morphostructural map		
The highest rank of lineament in a node, (HR)	2	1
Number of lineaments forming a node, (NL)	2	2
Distance to the nearest 1st rank lineament, km, (D1)	30	0
Distance to the nearest 2nd rank lineament, km, (D2)	0 20	28 45
Distance to the nearest node, km, (Dn)	15 20	20
D) Morphological parameter (Mor)		
This parameter is equal to one of the following six values in accord with the morphology within each node:	1.5	1.5
1 - mountain and plain (m/p)		
2 - piedmont and plain (pd/p)		
3 - plain only (p)	-65 -20	
E) Gravity parameters	-110 -85	-40
Maximum value of Bouguer anomaly, mGal, (Bmax)	30 50	-100 -60
Minimum value of Bouguer anomaly, mGal, (Bmin)		20 40
Difference between Bmax and Bmin mGal, (ΔB)		

The variants I and IV are discarded because too many nodes are assigned to class D; moreover, the variant IV also misses several nodes hosting target events. The variants II and III are practically equal, in spite of the difference in the learning sets D_0. Although the variant III misses

Table 3 - Results of recognition for nodes located in the Po Plain. The total number of nodes, both D and N, is 60. The total number of past earthquakes M5+ occurred within the nodes is 18.

Variants of classification obtained with different learning sets D_0	I All events from UCI catalogue are used to define D_0	II Nodes 28 (Milan) and 80 (Venice) are excluded from D_0	III Only nodes hosting events after 1500 are used to define D_0	IV D- and N-traits as defined for Iberia	V Nodes 54 and 101 (Emilia) are excluded from D_0
Total number of identified D nodes	32 (53%)	20 (33%)	20 (33%)	37 (62%)	20 (33%)
Total number of target earthquakes within the identified D nodes	18 (100%)	16 (89%)	13 (72%)	8 (44%)	12 (67%)

three nodes (namely 28, 80, 82), all hosting events occurred before 1500, it is considered the main variant, because to define D_0 only nodes hosting events M5+ that occurred after 1500 are used, when the epicentral locations in the UCI catalogue are relatively more reliable. Nevertheless, the location of the nodes 28, 80 and 82 (Fig. 2), which experienced M5+ earthquakes before 1500 (when the reliability of the epicentral locations is severely conditioned by the naturally limited amount of available information), close to important cities (Milan and Venice) calls for a deeper investigation that will be performed in a forthcoming study.

The Po Plain is generally characterized by moderate size earthquakes, with magnitudes not exceeding 5 for the majority of events. Nevertheless, there are some important exceptions. In 2012 the SE part of the Po Plain, region Emilia Romagna, was struck by the M=6.1 earthquake, which occurred at the node 54. The main classification of the nodes in the Po Plain presented in Fig. 3 has been obtained using the node hosting the 2012 Emilia Romagna earthquake for training the Cora-3 algorithm. To challenge the prediction capability of MZ_P we have made an experiment excluding node 54 from the learning set D_0. Even when it is excluded from D_0, the node 54 is still recognized as D. Therefore, the node hosting the May 20, 2012 Emilia Romagna earthquake could have been properly recognized as prone to $M \geq 5.0$ earthquakes.

Recognition of nodes related to first rank lineaments. Two variants of recognition, A and B have been obtained, using different learning sets D_0. In the variant A the set D_0 was formed using all the nodes situated most closely to the epicentres of past earthquakes M5+. In the variant B we excluded from D_0 three nodes 56, 75, 76 hosting events before 1500. The results of the recognition are presented in Table 4. In both variants, A and B, the same classification of the nodes into D and N classes is obtained. All the nodes hosting past earthquakes have been correctly recognized. Thus, each of the two variants can be considered as the main one.

The reliability of the recognition results has been evaluated by a set of control tests relevant to the determination of earthquake-prone areas (Gorshkov *et al*., 2003). We define as *main variants* the classification III presented in Table 3 and the classification B presented in Table 4.

Four tests have been performed to analyze the stability of the nodes classification obtained for each group of nodes, e.g., checking the recognition of specific nodes when they are excluded from the training set. The results of the tests performed support the validity of the main variants.

Based on the described pattern recognition procedure, the set of D nodes illustrated in Fig. 3 has been obtained, corresponding to the classification variant III for the Po Plain and variant B for the nodes related to the first rank lineaments.

Table 4 - Results of recognition for nodes located along the boundaries (1st rank lineaments) between the Po Plain and surrounding mountains. The total number of nodes, both D and N, is 42. The total number of past earthquakes M5+ occurred within the nodes is 53.

Classification variant	A All events from the UCI catalogue are used to select D_0	B Only nodes hosting events after 1500 are used to select D_0
Total number of identified D nodes	26 (62%)	26 (62%)
Total number of target earthquakes within the identified D nodes	52 (98%)	52 (98%)

4. Intermediate-term middle-range earthquake predictions based on precursory seismicity patterns

In addition to the recognition of areas prone to strong earthquakes [zero order or termless prediction: Keilis-Borok and Soloviev (2003)] we show that the application of pattern-recognition techniques permits to carry out a quantitative analysis of the dynamics of seismicity, aimed at the space-time identification of the priority areas, which are characterized by an increased probability of strong earthquake occurrence over the middle-range intermediate-term space-time scale.

Several possible scenarios of precursory seismic activity have been proposed; nevertheless, only a few formally defined algorithms allow for a systematic monitoring of seismicity, as well as for a widespread testing of their performances. Nowadays, one of the most promising approaches is represented by the intermediate-term middle-range earthquake predictions (i.e., with a characteristic alarm-time from a few months to a few years and a space uncertainty of hundreds of kilometres) based on the detection of formally defined variations in the background seismicity that precedes large earthquakes in a predefined area. In fact, the formal analysis of the seismic flow evidences that specific patterns in the events below some magnitude threshold, M_0, may prelude to an incumbent strong event, with magnitude above the same threshold M_0.

An essential step, when analyzing premonitory seismicity patterns, consists in the definition of the area where precursors have to be searched, the area of investigation, which is strictly interrelated with the size of the events to be predicted. For a natural reason, the size of the area should increase with the rupture size $L=L(M_0)$, where M_0 is the magnitude threshold. In particular, for the application of the methodology considered in this paper, it has been found empirically that the linear dimensions of the investigated area must be greater or equal to $5L$-$10L$. This condition is especially relevant in view of the Multiscale Seismicity (MS) model

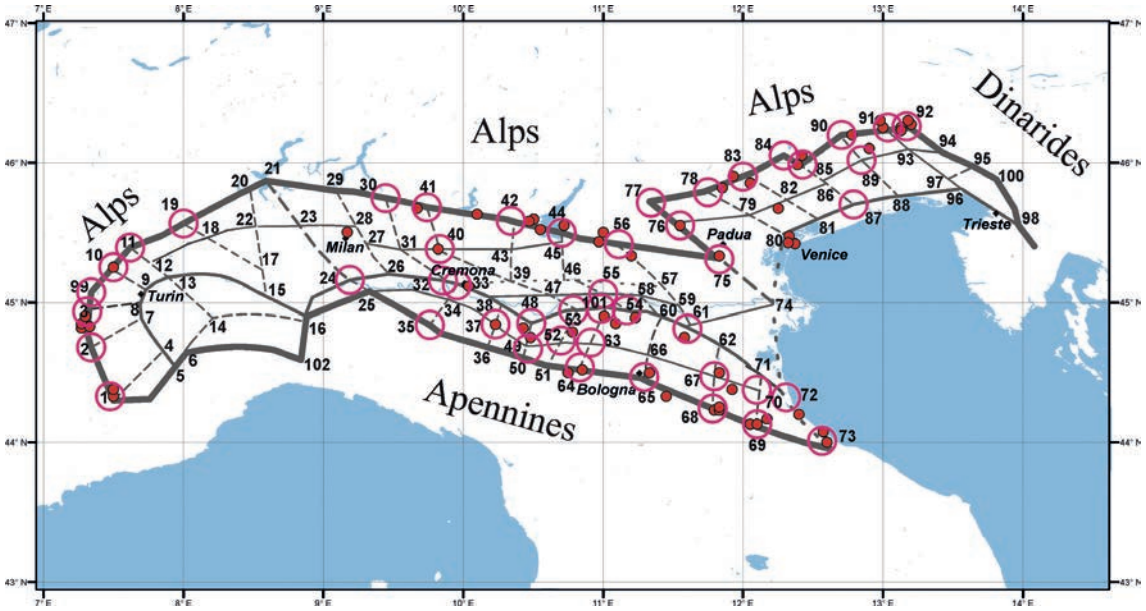

Fig. 3 - MZ map of the Po Plain and earthquakes M5+ from 1093 to 2012. Lines depict lineaments of different rank. Dots mark epicentres M5+ from the UCI catalogue. Red circles show recognized nodes prone to M5+ earthquakes.

(Molchan *et al*., 1997). In fact, according to the MS model, the Gutenberg-Richter (GR) relation can be considered a law that describes adequately only the ensemble of earthquakes that are geometrically small with respect to the dimensions of the analysed region. In agreement with the MS model, when seismicity is analyzed over relatively small regions, the frequency-magnitude relation is linear [i.e., can be related with the Self-Organised Criticality (SOC) paradigm] only up to a certain magnitude, while for the larger events it usually exhibits an upward bend. Specifically, within the areas delimited for prediction purposes, the number of earthquakes with $M>M_0$ (i.e., the target earthquakes, whose source size is comparable with the region size) usually exceeds the extrapolation of the GR law (i.e., does not follow SOC) and hence these events can be considered abnormally strong within the given region. At the same time the MS model guarantees the self-similarity condition for the small and moderate events ($M<M_0$) considered for the analysis of the premonitory patterns, and hence the log-linearity of the frequency-magnitude relation in the magnitude range of interest. In such a way, as discussed by Peresan *et al*. (2005), the algorithms make use of the information carried by the many small and moderate earthquakes, statistically obeying the GR law, to predict the strong earthquakes that do not satisfy the log-linearity of the GR law.

In this study two algorithms are considered, namely CN (Keilis-Borok and Rotwain, 1990) and M8 algorithms (Keilis-Borok and Kossobokov, 1990) that belong to a family of middle-range intermediate-term earthquake prediction algorithms based on a formalized, quantitative analysis of the seismic flow. The algorithms are based on a multiple set of premonitory patterns and have been designed following the general concepts of pattern recognition, which automatically imply strict definitions and reproducible prediction results. CN and M8 algorithms allow for a diagnosis of the Times of Increased Probability (TIPs) for the occurrence, inside a given region and time window, of earthquakes with magnitude greater than a fixed

threshold M_0. Quantification of the seismicity patterns is obtained through a set of empirical functions of seismicity, each representing a reproducible precursor, whose definition has been guided by the theory of complex system and laboratory experiments on rocks fracturing. Specifically, the functions, which are evaluated on the sequence of the main shocks occurred within the analyzed region, account for increased space-time clustering of moderate size earthquakes, as well as for specific changes in seismic activity, including anomalous activation and quiescence.

The simple definition of alarm periods as "Times of Increased Probability with respect to normal conditions", which are not associated to a specific value of probability for the occurrence of a strong earthquake, is imposed by the fact that any attempt to quantify precisely the probability increase during TIPs would require several a priori assumptions (i.e., Poissonian recurrence, independence of TIPs, etc.), most of which would be poorly constrained by the available observations. Although many researchers still concentrate their efforts on assigning probability values, it is well known that making quantitative probabilistic claims, particularly for large and infrequent events, requires a long series of recurrences, which cannot be obtained at local scale from the existing catalogues of earthquakes. Resorting to subjective probability assessment, e.g., by expert elicitation process, may misled to the impression of detailed knowledge, which often turns out wrong (e.g., Kossobokov, 2005, 2008, 2009). Anyway, decision-making does not necessitate a specific value of probability to be assigned, but rather requires an authoritative opinion on increased likelihood of incipient disaster (Anonymous, 1983). Thus, from a practical point of view, a hierarchical step-by-step approach to earthquake predictions (e.g., Kossobokov and Shebalin, 2003) appears preferable that ranges from term-less recognition of earthquake prone areas, to intermediate-term and, possibly, to short-term alerts. This multi-scale approach may benefit, at any stage, from independent complementary evidence from space geodesy, geochemical and other geophysical observations (Kanamori, 2003; Bormann, 2011; Panza *et al*. 2011).

The tests of predictions, performed on a global scale, already allowed for a statistical assessment of the predictive capability of M8 and CN algorithms, as confirmed by ICEF Report (Jordan *et al*., 2011). Specifically, for the M8 algorithm the on-going real-time prediction experiment, started in 1992 (Healy *et al*., 1992) for the great (M8.0+) and major (M7.5+) earthquakes worldwide (see http://mitp.ru/en/default.html), already demonstrated the high confidence level (above 99%) of the results (Kossobokov, 2012). For the algorithm CN a preliminary estimate of the significance of the prediction results, obtained for the period 1983-1998 in 22 regions of the world, provided a confidence level around 95% (Rotwain and Novikova, 1999). Such conclusions are supported by the statistically significant results obtained by the rigorous prospective testing of CN and M8S algorithms over the Italian territory (Peresan *et al*., 2011), ongoing for more than a decade, as described in this paper.

5. Prospective testing of CN and M8S predictions in Italy

Italy is the only region of moderate seismic activity where the two algorithms CN and M8S are currently applied simultaneously for the routine intermediate-term middle-range earthquake prediction (Peresan *et al*., 2005). Significant efforts have been made to minimize the intrinsic

space uncertainty of predictions and the subjectivity of the definition of the areas where precursors should be identified (Peresan *et al*., 1999; Kossobokov *et al*., 2002). For the application of the algorithm CN, a regionalization strictly based on the seismotectonic zoning, and taking into account the main geodynamic features of the Italian area, is currently used (Peresan *et al*., 1999, 2011), as shown in Fig. 4. For the application of the M8S algorithm (Kossobokov *et al*., 2002), that is a spatially stabilized variant of M8, the seismicity of the study region is analyzed within a dense set of overlapping circles [the circles of investigation (CIs)], with radius increasing with increasing magnitude of the target events, that cover the monitored area. A hierarchy of predictions is delivered for different magnitude ranges M_0+, considering values of M_0 with an increment of 0.5 (i.e., M_0+ indicates the magnitude range: $M_0 \leq M \leq M_0+0.5$). In Italy M8S predictions are performed in the three different magnitude ranges defined by M6.5+, M6.0+ and M5.5+, with CIs of radius R=192 km, R=138 km, and R=106 km, respectively.

Several experiments have been dedicated to assess the robustness of the methodology against the unavoidable uncertainties in the data (Peresan *et al*., 2000, 2002). With these results acquired, a still ongoing experiment has been launched in July 2003, aimed at the rigorous real-time prospective testing of M8S and CN prediction for earthquakes with magnitude larger than a given threshold (namely 5.4 and 5.6 for CN algorithm, and 5.5 for M8S algorithm) in the Italian region and its surroundings. The goal of the experiment is to accumulate a collection of correct and wrong predictions (the latter include the false alarms and/or the failures to predict encountered in the test) permitting to verify and assess the predictive capability of the considered methodology. In this framework, CN and M8S predictions have been routinely updated according to a predefined schedule, that is every two months CN predictions (i.e., on January, March, May, July, September, November) and every six months M8S predictions (i.e., on January and July). The rules for the real-time application of CN and M8S algorithms to the Italian territory are described in detail in Peresan *et al*. (2005).

The routinely updated predictions and a complete archive of predictions are made available on-line via the following website: http://www.geoscienze.units.it/esperimento-di-previsione-dei-terremoti-mt.html, thus allowing for rigorous validation and independent evaluation of the applied algorithms. The full list of target earthquakes for CN and M8S algorithms, both in retrospective and real-time application in Italy and adjacent territory, is provided in Tables 5 and 6, respectively. The operating magnitude for M8S algorithm is the maximum magnitude, M_{max}, whereas for CN application M_{prio} is considered, i.e., for each event, among the different magnitudes listed in the catalogue one is selected according to the priority criteria described in Peresan *et al*. (2005).

The results obtained so far, summarized in Tables 7 and 8, already permitted a preliminary assessment of the significance of the issued predictions by real-time monitoring (Peresan *et al*., 2011, 2012). All together 13 out of the 15 target earthquakes, occurred within the monitored territory since 1963, have been correctly preceded by an alarm (TIP) declared by CN algorithm. About 30% of the overall space-time volume (STV) is occupied by alarm and the confidence level of such predictions is above 99%. Similarly, the algorithm M8S correctly identified 14 of the 23 earthquakes with magnitude M5.5+ (i.e., between 5.5 and 6.0), occurred since 1972 within the monitored territory, with a STV of alarm of about 31%; the confidence level of M5.5+ predictions is above 98% (no estimation is yet possible for higher magnitude levels, due to the limited number of target events).

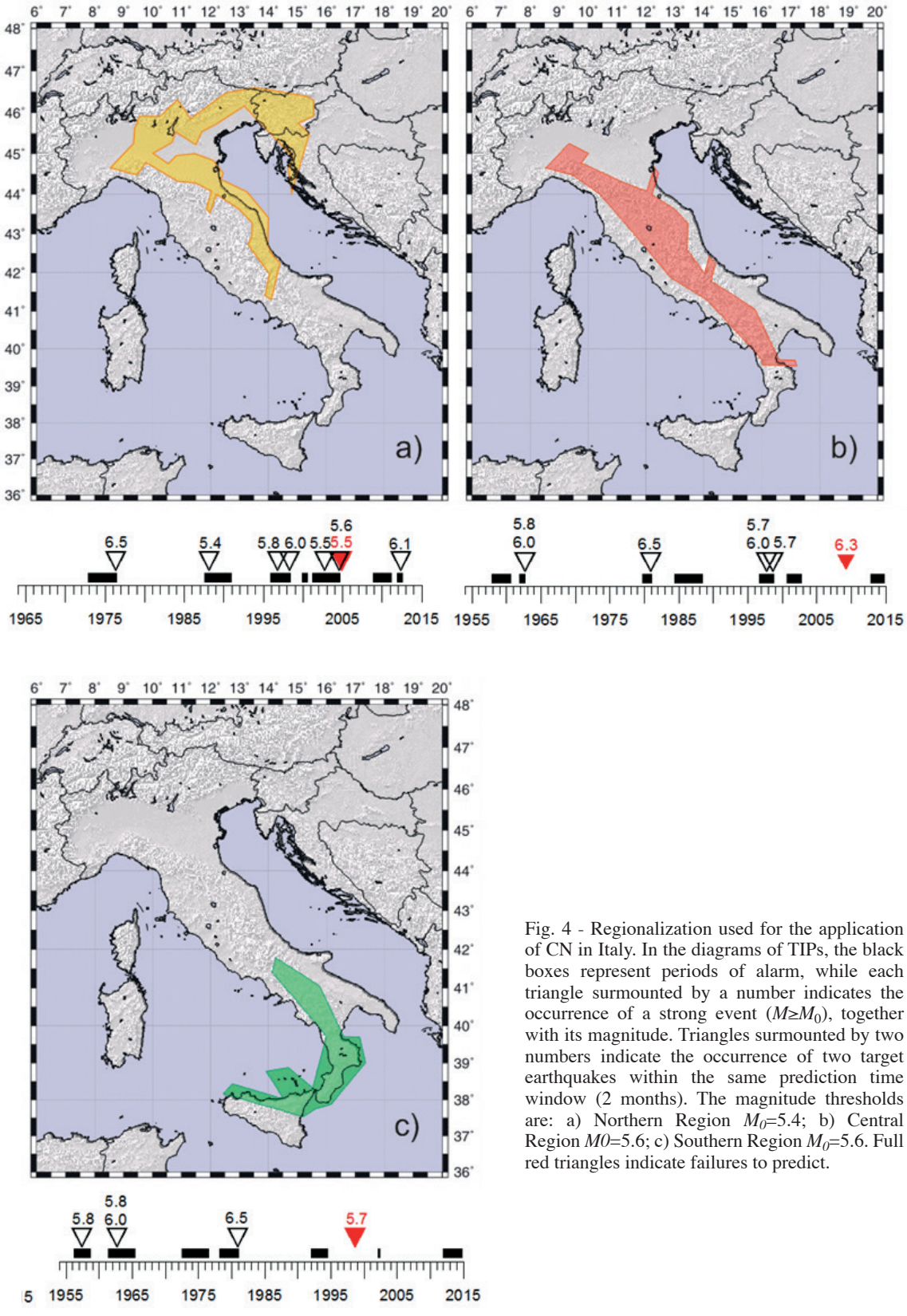

Fig. 4 - Regionalization used for the application of CN in Italy. In the diagrams of TIPs, the black boxes represent periods of alarm, while each triangle surmounted by a number indicates the occurrence of a strong event ($M \geq M_0$), together with its magnitude. Triangles surmounted by two numbers indicate the occurrence of two target earthquakes within the same prediction time window (2 months). The magnitude thresholds are: a) Northern Region M_0=5.4; b) Central Region $M0$=5.6; c) Southern Region M_0=5.6. Full red triangles indicate failures to predict.

Particularly relevant appears the high confidence level of the real-time prediction experiment. Specifically, since the beginning of prospective testing, 5 out of 7 target earthquakes have been predicted in real-time by CN with about 30% STV of alarms; M8S algorithm predicted 5 out of 9 earthquakes with a STV of alarms as low as 14% of the total monitored space-time volume; the probability of obtaining such results by random guess is below 3%. The space-time volume of alarms is computed accounting for the rate of occurrence of past earthquakes in the area under investigation [Relative Intensity (RI)], following the procedure described by Kossobokov *et al*. (1999). The STV measure based on the seismicity distribution is more stringent than the measure based on simple spatial extent (in kilometres) of alarm areas, and allows for the assessment of the significance of the issued predictions with respect to a time-independent and non-clustered seismicity model (i.e., RI), according to which future large earthquakes are considered more likely where higher seismic activity occurred in the past.

Table 5 - List of target earthquakes for CN retrospective (1954-1997) and real-time (1998-2014) application in Italy and adjacent territory. The earthquakes occurred during the period of forward monitoring, since 1998, are evidenced in bold.

Date	Latitude °N	Longitude °E	Depth	M_{prio}	CN	CN Region
1957.05.20	38.70	14.10	60	5.8	Yes	South
1962.08.21	41.15	15.00	40	6.8	Yes	Centre, South
1962.08.21	41.15	15.00	40	6.0	Yes	Centre, South
1976.05.06	46.23	13.13	12	6.5	Yes	North
1980.11.23	40.85	15.28	18	6.5	Yes	Centre, South
1988.02.01	46.31	13.13	8	5.4	Yes	North
1996.10.15	44.79	10.78	10	5.8	Yes	North
1997.09.26	43.08	12.81	10	5.7	Yes	Centre
1998.04.12	**46.24**	**13.65**	**10**	**6.0**	**Yes**	**North**
1998.09.09	**40.03**	**15.98**	**10**	**5.7**	**Yes**	**Centre, South**
2003.09.14	**44.33**	**11.45**	**10**	**5.6**	**Yes**	**North**
2004.07.12	**46.30**	**13.64**	**7**	**5.7**	**Yes**	**North**
2004.11.24	**45.63**	**10.56**	**17**	**5.5**	**No**	**North**
2009.04.06	**42.33**	**13.33**	**8**	**6.3**	**No**	**Centre**
2012.05.20	**44.90**	**11.23**	**6**	**6.1**	**Yes**	**North**

* Only the Central and Southern regions are considered up to 1964.

Table 6 - List of target earthquakes for M8S retrospective (1972-2001) and real-time (2002-2014) application in Italy and adjacent territory. Three magnitude ranges are considered: M6.5+, M6.0+, M5.5+. The earthquakes occurred during the period of forward monitoring are evidenced in bold.

Date	Latitude °N	Longitude °E	Depth	Mmax	M8S	Commentary
M6.5+						
1976.05.06	46.23	13.13	12	6.5	Yes	
1980.11.23	40.85	15.28	18	6.7	Yes	
M6.0+						
1997.09.26	43.08	12.81	10	6.4	No	Predicted in M5.5+
1998.04.12	46.24	13.65	10	6.0	Yes	Slovenia
2009.04.06	**42.33**	**13.33**	**8**	**6.3**	**No**	
2012.05.20	**44.90**	**11.23**	**6**	**6.1**	**No**	
M5.5+						
1975.01.16	38.20	15.78	21	5.5	Yes	
1978.04.15	38.27	15.10	18	5.8	Yes	
1979.09.19	42.72	12.95	6	5.8	No	20 km from alarm
1980.05.28	38.46	14.34	19	5.5	Yes	
1986.11.25	44.12	16.34	30	5.5	No	Croatia
1990.05.05	40.78	15.77	10	5.6	Yes	
1990.11.27	43.85	16.63	24	5.6	No	Croatia
1991.02.26	40.19	13.82	401	5.5	No	Deep event
1994.01.05	39.08	15.15	272	5.8	No	Deep event
1996.10.15	44.79	10.78	10	5.8	Yes	
1997.09.26	43.05	12.88	10	5.9	Yes	
1998.05.18	39.25	15.11	279	5.6	Yes	Deep event
1998.09.09	40.03	15.98	10	5.9	Yes	
2001.07.17	46.73	11.20	10	5.5	Yes	
2002.09.06	**38.38**	**13.70**	**5**	**5.9**	**No**	
2002.10.31	**41.79**	**14.87**	**10**	**5.9**	**No**	
2003.03.29	**43.11**	**15.46**	**10**	**5.5**	**Yes**	
2003.09.14	**44.33**	**11.45**	**10**	**5.6**	**Yes**	
2004.02.23	**47.27**	**6.27**	**17**	**5.5**	**Yes**	**Switzerland**
2004.05.05	**38.51**	**14.82**	**228**	**5.5**	**No**	**Deep event**
2004.07.12	**46.30**	**13.64**	**24**	**5.6**	**No**	**Slovenia**
2004.11.24	**45.63**	**10.57**	**24**	**5.5**	**Yes**	
2006.10.26	**38.67**	**15.40**	**216**	**5.8**	**Yes**	**Deep event**
2009.04.06	**42.33**	**13.33**	**6**	**6.3**	**No**	

Table 7 - Space-time volume of alarm for CN application in Italy. *N* is the total number of target events, while *n* is the number of predicted earthquakes. During the period 1954-1963 only the Central and Southern regions were analyzed.

Experiment	Space-time volume of alarm (%)	*n/N*	Confidence level (%)
Retrospective* (1954 - 1963)	41	3/3	93
Retrospective (1964 - 1997)	27	5/5	>99
Forward (1998 - 2014)	30	5/7	97
All together (1954 - 2014)	30	13/15	>99

Table 8 - Space-time volume of alarm for M8S application in Italy, for the three magnitude ranges defined by M6.5+, M6.0+ and M5.5+. *N* is the total number of target events, while *n* is the number of predicted earthquakes. The confidence level of forward predictions for M5.5+ is above 99%.

Experiment	M6.5+		M6.0+		M5.5+	
	Space-time volume of alarm (%)	*n/N*	Space-time volume of alarm (%)	***n/N***	Space-time volume of alarm (%)	***n/N***
Retrospective (1972 - 2001)	35	*2/2*	39	1/2	38	9/14
Forward (2002 - 2014)	24	*0/0*	31	0/2	14	5/9
All together (1972 - 2014)	31	*2/2*	36	1/4	31	14/23

The uncertainties associated with intermediate-term middle-range earthquake predictions are intrinsically quite large; CN and M8S algorithms, however, already proved effective in predicting strong earthquakes, by rigorous prospective testing over the Italian territory. The increase in probability of strong earthquake occurrence associated with the alarmed areas (TIPs) can be grossly estimated based on the results obtained so far. The results from such analysis are summarized in Table 9. The yearly probability for a target earthquake occurrence within one of the CN monitored regions varies from 8% to 16%, depending on the region. When taking into account predictions, i.e., considering only the alerted time intervals (TIPs), such probability increases up to 24% and 48% respectively; accordingly, it is possible to quantify the probability gain associated with a TIP. Similarly, the probability for a target earthquake to occur, when no TIP is diagnosed, can be estimated around 2-3%. In all cases, the conditional probability, estimated accounting for the CN results, differs significantly from the average probability of target earthquakes occurrence within each of the monitored regions. This fact evidences the predictive capability of the algorithm. Moreover, in the diagram of time distribution of alarms (TIPs) reported in Fig. 4 it is possible to observe that the false alarm rate ranges from 30% for CN in the Northern Region to about 50-60% in the Southern Region (Table 9); in several cases the false alarms are associated with the continuation of a TIP after the occurrence of a strong earthquake.

Based on similar reasoning, we have estimated the relative frequency of target earthquakes, which occurred within the entire space-time volume monitored by CN and M8S algorithms, and we have compared this estimate with that associated with the alerted volume (based on Tables 7 and 8). The frequency of target events turns out significantly higher within alarmed STV; namely, the frequency increases by about a factor 3 within the alarmed periods, when compared to the long term average rate. Accordingly, the probability gain associated with CN and M8S predictions for the Italian territory can be grossly estimated between 2 and 4, in good agreement with the independent estimates by ICEF (Jordan *et al*., 2011). Noticeably, these conclusions are based rigorously on the results from real-time prospective testing of the considered prediction algorithms, and thus reflect their effective predictive capability.

The operational effectiveness, along with the statistical validation, is a key element in the assessment of any earthquake prediction method; hence it should be properly defined and analyzed, avoiding approximate and incomplete representations, which often overlook the wide spectrum of possible mitigation actions [e.g., ICEF report, Jordan *et al*. (2011); Kossobokov *et al*. (2015)].

Although the predictive capability of the considered algorithms, with respect to a random Poissonian model, has been clearly recognized, it would be interesting to compare CN and M8S predictions against models based on earthquake clustering. However, so far no rigorously validated clustering model for the Italian territory is available to us to carry out such analysis, since the assessment for most of the clustering models is currently based on retrospective results and nominal probability gains. The prediction experiment by CN and M8S algorithms are, in fact, the only formally validated tools capable to anticipate the occurrence of strong earthquakes in the Italian region. CN and M8S prediction experiments started much earlier than the model testing within the Collaboratory for the Study of Earthquake Predictability - Testing Region Italy, CSEP-TRI (i.e., August 2009; http://cseptesting.org/regions/italy) that has, so far, not released any document on the results achieved by prospective testing.

Table 9 - Analysis of the relative frequency of target earthquakes within the three regions monitored by CN algorithm (Fig. 4) in the period 1954-2014.

		Number of events	Time (years)	Time %	Yearly probability %	Gain	False/Total alarms
NORTH	All time	8	49,86	100	16	3,0	3/10
	Alarm	**7**	**14,66**	**29**	48		
	No Alarm	1	35,20	71	3		
CENTRE	All time	7	59,92	100	12	3,9	4/8
	Alarm time	**6**	**13,23**	**22**	45		
	No Alarm	1	46,69	78	2		
SOUTH	All time	5	59,92	100	8	2,9	5/9
	Alarm time	**4**	**16,73**	**28**	24		
	No Alarm	1	43,19	72	2		

5.1 Analysis of the stability of prediction results

In addition to the standard monitoring of precursory seismicity patterns, performed according to the rules defined in Peresan *et al.* (2005), a set of stability tests, with respect to the input earthquake catalogues, has been accomplished. A detailed description of the UCI earthquake catalogue (Peresan and Panza, 2002), used for the routine monitoring of seismicity by CN and M8S algorithms, is available at: http://www.geoscienze.units.it/esperimento-di-previsione-dei-terremoti-mt/the-italian-earthquakes-catalogue/124-description-of-the-catalogue-.html. Due to a remarkable incompleteness detected for the NEIC Preliminary Determinations of Epicenters since January 2009, the earthquake catalogue UCI is currently updated using the NEIC data integrated by ISC bulletins information (starting on January 2012).

A preliminary comparative analysis of the different instrumental earthquake catalogues for the Italian territory, made available in the framework of the CSEP-TRI experiment, has been carried out. The analysis evidenced the existence of relevant heterogeneities in the different instrumental data sets (Romashkova *et al.*, 2009; Romashkova and Peresan, 2013), which should be taken into account when using them for the analysis of seismicity. The detected magnitude changes, in fact, may obscure possible precursory seismicity patterns or, in turn, may introduce spurious variations in reported seismicity, not related to any underlying physical process. The heterogeneous magnitude estimates provided over different time spans,

therefore, prevent the use of the CSEP-TRI instrumental earthquake catalogues for CN and M8S algorithms testing in the Italian territory. The magnitude heterogeneity detected so far by Romashkova *et al*. (2009), has been recently corroborated by independent analysis by Gasperini *et al*. (2013). This observation poses serious concern on the results that could be obtained from CSEP-TRI testing based on such input data, as already evidenced by Peresan *et al*. (2012).

5.1.1. Stability tests with respect to different input earthquake catalogues

Some experiments have been performed to assess the possibility of updating CN and M8S predictions using the Bollettino Sismico Italiano (BSI) data since 2005. The BSI, in fact, is the authoritative catalogue to be used for CSEP testing over the Italian territory (CSEP-TRI); remarkably such bulletins are available only starting from April 2005, whereas earlier data [i.e., bulletins from ISIDe website (ISIDE Working Group, 2015)] are discontinuous and heterogeneous, as described by Romashkova and Peresan (2013).

Specifically, the variability of prediction results has been tested against the use of different input data, namely using the UCI catalogue and the catalogue obtained updating UCI by the BSI bulletins since April 16, 2005 (referred as UCI+BSI in the following). The results of such experiments, provide essential information for the assessment of the possible operational use of BSI data for real-time prediction testing, as described hereinafter.

By the straightforward comparison of the annual number of earthquakes above different magnitude thresholds (Fig. 5), a clear magnitude discrepancy can be observed between the UCI and BSI data in the period of their overlapping, namely 2005-2012. The BSI magnitudes are systematically lower than those from UCI. The discrepancy seems to increase for larger earthquakes. The frequency-magnitude graphs (Fig. 6) calculated for UCI for the periods before and after April 16, 2005, and for BSI catalogue since April 16, 2005 confirm that BSI magnitudes are systematically lower than those reported in UCI catalogue for the corresponding earthquakes.

Therefore, it is natural to conclude that the straightforward updating of UCI by BSI starting from April 16, 2005 is not appropriate, in case the catalogue is intended to be used for prediction purposes. Having this problem in mind, a test application of M8S algorithm has been performed using the UCI+BSI data, in order to check the variability of the results with varying input catalogue. Since the area of CSEP region is smaller than that of standard M8S experiment for Italy and its surroundings, the M8S code has been modified to be applied to this restricted area. The results of the standard and modified M8S tests, where the data of UCI and UCI+BSI catalogues are used, show that the outputs are different, although some similarity in alarm areas exists. In general, the space-time volume of alarm in M8S-CSEP test (i.e., considering CSEP region and UCI+BSI catalogue) is smaller than that in the standard one, for all of the three magnitude ranges.

Similar results have been obtained for CN application using the composite UCI+BSI catalogue. The analysis of the frequency-magnitude distributions within individual CN regions evidenced certain spatial heterogeneity; with data discrepancies particularly relevant within the CN Southern Region. As a result, when using UCI+BSI catalogue an increase in the STV of alarms is observed for the Central Region, while in the Northern and Southern regions the STV is reduced at the cost of additional failures to predict. Thus, the use of BSI data causes a

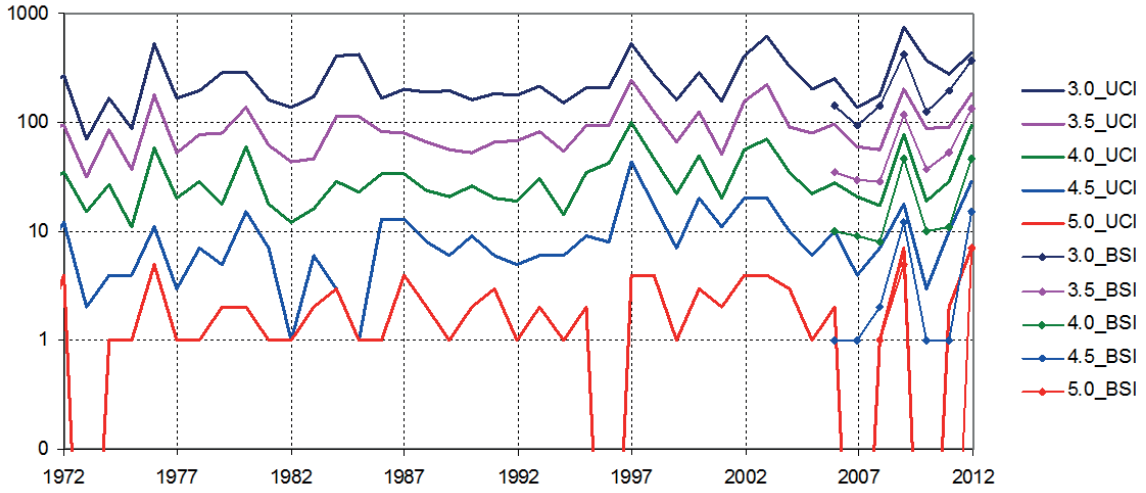

Fig. 5 - Annual number of earthquakes above different magnitude thresholds versus time in the two data sets: UCI, 1972-2012, and BSI, 2005-2012. Both are selected for CSEP collection region, depth 0-30 km.

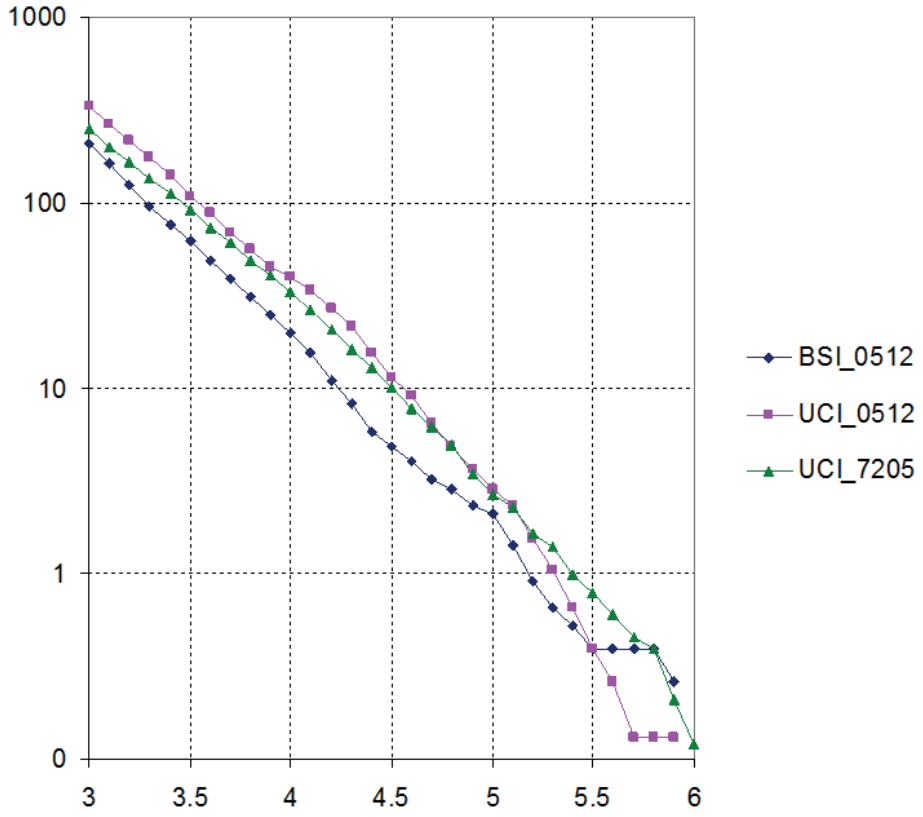

Fig. 6 - Annual frequency-magnitude graphs for two catalogues in different time intervals: BSI, 2005.04.16-2012; UCI, 2005.04.16-2012, and UCI, 1972-2005.04.15.

deterioration of prediction results, with respect to those obtained by the rigorous prospective testing, based on UCI catalogue alone. Although the short time span of BSI data availability (about ten years) does not allow for a reliable assessment of the related predictions, the results of the preliminary data analysis and the test applications do not support the use of BSI data for the update of UCI on regular basis.

6. Neo-deterministic time-dependent seismic hazard scenarios for the Italian territory

A reliable and comprehensive characterization of expected seismic ground shaking, eventually including the related time information, is essential in order to develop effective mitigation strategies and increase earthquake preparedness. Moreover, any effective tool for seismic hazard assessment must demonstrate its capability in anticipating the ground shaking related with large earthquake occurrences, a result that can be attained only through rigorous verification and validation process against the real seismic activity.

The procedure for the neo-deterministic seismic zoning, NDSHA, is based on the calculation of realistic synthetic seismograms, as described in detail in Panza *et al*. (2012). Starting from the available information on the Earth structure, seismic sources, and the level of seismicity of the investigated area, ground motion is defined by full waveform modelling. Hence, the method does not make use of attenuation models, which may be unable to account for the complexity of the medium and of the seismic sources (Paskaleva *et al*., 2007), and are often poorly constrained by the available observations (e.g., Burger *et al*., 1987; Panza and Suhadolc, 1989; Fäh and Panza, 1994; Bragato *et al*., 2011). NDSHA, in its standard form, defines the hazard as the maximum ground shaking at the site, computed considering a large set of scenario earthquakes, including the maximum credible earthquake, associated with the different sites. Seismic sources considered for ground motion modelling are defined based on the largest events reported in the earthquake catalogue, as well as incorporating the additional information about the possible location of strong earthquakes provided by the morphostructural analysis, active fault studies and other geophysical indicators (including GPS observations), thus filling in gaps in known seismicity (Panza *et al*., 2011).

Based on NDSHA approach, an operational integrated procedure for seismic hazard assessment has been developed that allows for the definition of time-dependent scenarios of ground shaking, through the routine updating of earthquake predictions, performed by means of CN and M8S algorithms (Peresan *et al*., 2011). The integrated NDSHA procedure for seismic input definition, which is currently applied to the Italian territory, combines the different pattern recognition techniques, designed for the space-time identification of strong earthquakes, with algorithms for the realistic modelling of ground motion. Accordingly, a set of deterministic scenarios of ground motion at bedrock, proper for the time interval when a strong event is likely to occur within the alerted areas can be defined by means of full waveform modelling, both at regional and local scale.

In Italy and surrounding regions the areas prone to strong earthquakes ($M \geq 6.0$ and $M \geq 6.5$) have been systematically identified based on the morphostructural zonation and pattern recognition analysis (Gorshkov *et al*., 2002, 2004), according to the procedure described in

section 1. The identified seismogenic nodes are used, along with the seismogenic zones ZS9 (Meletti and Valensise, 2004), to characterize the earthquake sources used in the seismic ground motion modelling, as described by Peresan *et al*. (2011). The earthquake epicentres reported in the catalogue are grouped into 0.2°x0.2° cells, and to each cell the maximum magnitude, recorded within it, is assigned. A smoothing procedure is then applied, to account for spatial uncertainty and for source dimensions. Only the sources located within the alarmed areas are considered to define the time-dependent scenarios.

Synthetic seismograms are, then, computed for sites placed at the nodes of a grid with step 0.2°x0.2° that covers the national territory, considering the average structural model associated to the regional polygon that includes the site. The seismograms used to be computed for an upper frequency content of 1 Hz, that is consistent with the level of detail of the regional structural models, and the point sources are scaled for their dimensions using the spectral scaling laws proposed by Gusev (1983), as reported in Aki (1987). From the set of complete synthetic seismograms, different maps of seismic hazard that describe the maximum ground shaking at the bedrock can be produced, including peak ground displacement (*PGD*), velocity (*PGV*) or design ground acceleration (*DGA*).

NDSHA has been recently extended to frequencies as high as 10 Hz; the preliminary results from this ongoing research (i.e., the regression relations between the strong motion parameters and the macroseismic intensities), basically confirm the results obtained with a 1 Hz cut-off frequency in the point-source approximation (Panza *et al*., 2012). On account of the available information about structural models and on the definition of damaging potential (Uang and Bertero, 1990; Decanini and Mollaioli, 1998) we consider, at the present stage of knowledge, the computation of velocities (10 Hz cut off frequency) the most stable and representative parameter to synthetically represent hazard. The scenarios of peak ground velocity associated with the three CN regions (Fig. 4) are illustrated in Fig. 7.

6.1 Prospective testing of time-dependent seismic hazard scenarios

CN and M8S predictions, as well as the related time-dependent ground motion scenarios associated with the alarmed areas, are routinely updated every two months since 2006. The procedure for the definition of the related ground shaking scenarios is illustrated in Peresan *et al*. (2011).

A strong earthquake (M_W=6.1) hit the Emilia Region, northern Italy, on May 20, 2012. The epicentre was localized inside the Northern Region (Fig. 4), alerted by CN algorithm for an earthquake with magnitude $M \geq 5.4$, starting on March 1, 2012, whereas it occurred outside the areas alerted by M8S algorithm for the corresponding magnitude interval. Therefore, the earthquake scores as a successful real-time prediction, for CN algorithm only. The time-dependent ground shaking scenario associated to CN Northern Region (Fig. 7a) defined for the period March 1, 2012 - May 1, 2012, correctly predicted the ground shaking, as large as ~0.25 g, recorded for this earthquake. Notably, the ground shaking for this earthquake systematically exceeded the values expected at the bedrock in the area according to current Italian seismic regulation (i.e., PGA<0.175 g), which is based on a classical PSHA map (Gruppo di Lavoro MPS, 2004).

Since the time NDSHA time-dependent scenarios are regularly computed, namely starting on 2006, this is the second large earthquake that struck the Italian territory, along with the

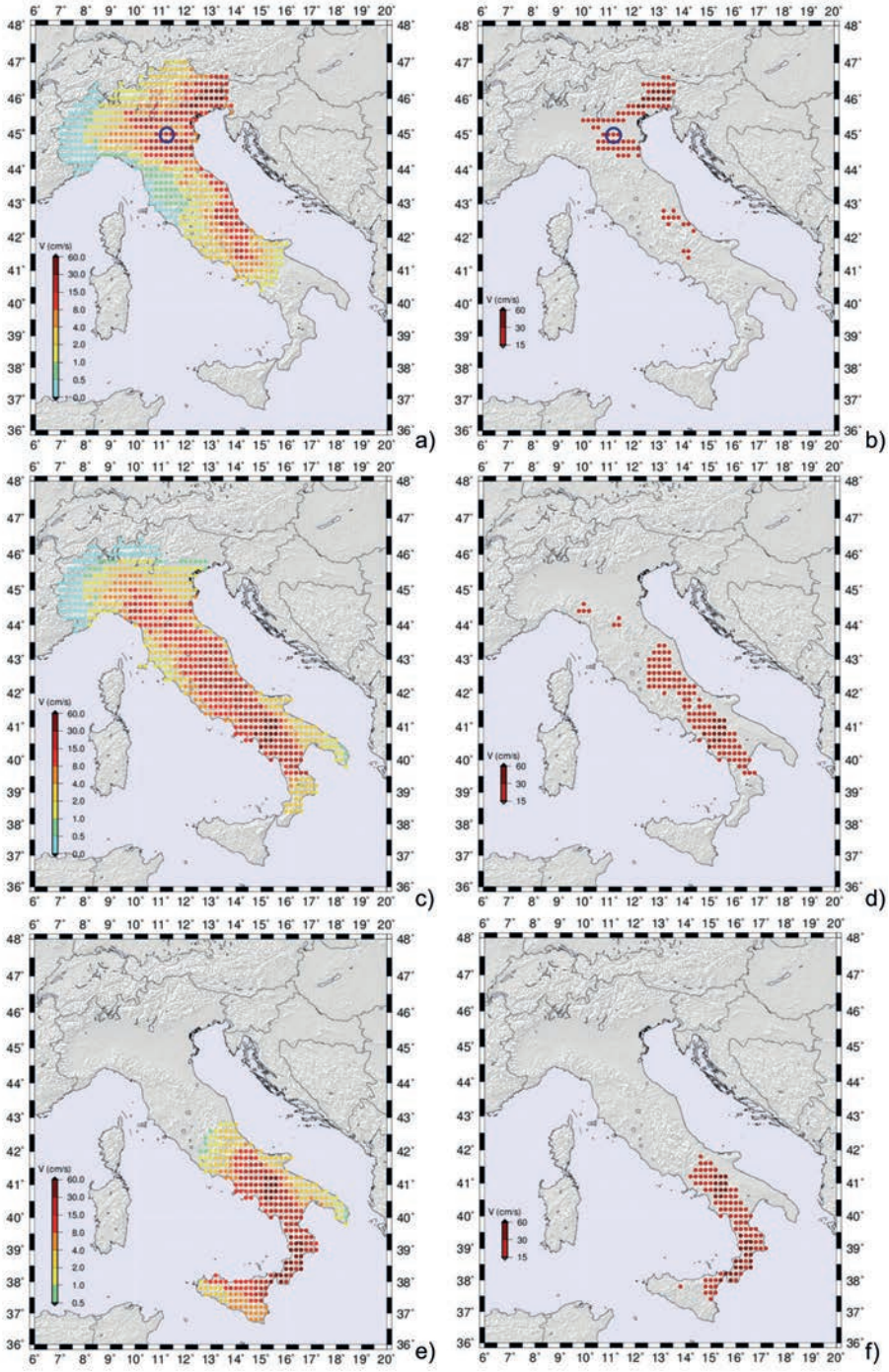

Fig. 7 – Time-dependent scenarios of ground shaking associated to an alarm in one of the monitored CN regions (Fig. 4). On the left column acceleration maps are shown, computed using simultaneously all of the possible sources within the alarmed area and for frequencies up to 10 Hz. On the right, the same maps are provided, but for *PGV*>15 cm/s. The circle on maps a) and b) evidences the area within 30 km distance from the epicentre of the 2012 Emilia earthquake (*M*=6.1). According to Table 9, when the alarm is declared, the probability associated with these scenarios ranges from 48% (Northern Region,) to 24% (Southern Region); when the alarm is off the corresponding probabilities are around 2-3%. Without accounting for predictions, the time-independent probabilities range from 8% to 16%, depending on the monitored region.

2009 L'Aquila earthquake (M=6.3). In both cases the method correctly predicted the observed ground motion, although L'Aquila earthquake scores as a failure in the earthquake prediction experiment, because the epicentre was located about 10 km outside the alarmed territory (Panza *et al.*, 2009; Peresan *et al.*, 2011).

The results acquired in the prospective application of the time-dependent NDSHA approach allow for a rigorous validation of the integrated methodology and, at the same time provide information that can be useful to assign unbiased priorities for timely mitigation actions. As an example, for sites where ground shaking values greater than 0.2 g are estimated at bedrock (Fig. 7), further investigations can be performed taking into account the local soil conditions, to assess the performances of relevant structures, such as historical and strategic buildings (e.g., Vaccari *et al.*, 2009) in addition to natural low key actions as described in Kantorovich and Keilis-Borok (1991).

The results presented in this section show that NDSHA permits to account for the temporal information about earthquakes occurrence provided by formally defined and tested tools for earthquake prediction. In addition, NDSHA can adequately address earthquake recurrence because it can naturally separate ground shaking from related recurrence (e.g., Panza *et al.*, 2014), contrary to PSHA, which strictly depends on assumptions about the recurrence of large earthquakes that have large uncertainties and often turn out to be incorrect. Although temporal information may play a role in preparedness actions, a dilemma arises when accounting for it in the formulation of building codes. In PSHA, for example, the predicted ground shaking depends on the relative lengths of the time window used (i.e., on the probability threshold selected) and the recurrence time between large earthquakes. By forecasting the expected value of ground shaking over a time interval, PSHA underpredicts the actual shaking if earthquakes with longer recurrence times occur; such underestimates propagate non-linearly into unbearable errors in the expected human and economic losses (Wyss *et al.*, 2012).

A comparative analysis among past seismicity, bedrock maps by NDSHA and by PSHA (reference for current seismic regulation) has been carried out for the Italian territory. Remarkably, the PSHA expected ground shaking estimated with 10% probability of being exceeded in 50 years (corresponding a return period of 475 years) appears underestimated (by about a factor 2) with respect to NDSHA estimates, particularly for the largest values of *PGA* (Zuccolo *et al.*, 2011). At the same time, the probabilistic maps have a higher tendency to overestimate the hazard, with respect to available observations, particularly in low-seismicity areas. Therefore, the predictive capability of the PSHA maps turns out quite unsatisfactory, as shown by Nekrasova *et al.* (2014).

7. Discussion and conclusions

We have shown, by rigorous prospective testing, that pattern recognition techniques proved effective in characterizing the space and time properties of impending strong earthquakes. The uncertainties associated with intermediate-term middle-range earthquake predictions are intrinsically quite large; however, they can be reduced by the combined use of independent information, including morphostructural and ground shaking information. Pattern recognition procedures, in fact, can be used to focus the investigation of possible local scale precursors

in the areas (with linear dimensions of few tens kilometres), where the probability of a strong earthquake is relatively high, as well as for deriving time-dependent scenarios of ground shaking by the NDSHA approach (Peresan *et al*., 2011).

The recognized earthquake prone areas provide the first-order systematic information that may significantly contribute to reliable seismic hazard assessment in the Italian territory, as shown by Zuccolo *et al*. (2011). The new indications about the seismogenic potential obtained from this study, although less accurate than detailed fault studies, have the advantage of being independent from past seismicity, since they rely on the systematic and quantitative analysis of the available geological and morphostructural data. Even if past earthquakes are considered in the selection of traits typical for areas prone to large earthquakes (i.e., in the "learning stage"), the seismogenic nodes recognition is based on a set of parameters, like elevation and thickness of sediments, which do not include seismicity. Thus, this analysis appears particularly useful in areas where historical information is scarce; special attention should be paid to dangerous seismogenic nodes that are not yet related with known active faults or past earthquakes.

The information about the possible location of strong earthquakes provided by the morphostructural analysis can be directly incorporated in the neo-deterministic procedure for seismic hazard assessment, thus filling in possible gaps in known seismicity (Panza *et al*., 2012). Moreover, the space information about earthquake prone areas can be fruitfully combined with the space-time information provided by the quantitative analysis of the seismic flow, so as to identify the priority areas (with linear dimensions of few tens kilometres), where the probability of a strong earthquake is relatively high (Panza *et al*., 2011; Peresan *et al*., 2011), for detailed local scale studies.

The described procedure for the definition of time-dependent seismic hazard scenarios, based on pattern-recognition techniques and ground motion modelling, has been implemented within the framework of the SISMA project (http://sisma.galileianplus.it/) of the Agenzia Spaziale Italiana, an integrated prototype system for real-time joint processing of seismic and geodetic data streams (Crippa *et al*., 2008; Panza *et al*., 2011). The SISMA prototype is a fully formalized and highly automated tool (including version control for software and products) for the systematic real-time monitoring of deformations and seismicity patterns, which was made available to the Civil Defence of the Friuli Venezia Giulia Region for independent testing.

The routine application of the time-dependent NDSHA approach provides information that can be useful in assigning unbiased priorities for timely mitigation actions and, at the same time, allows for a rigorous prospective validation of the proposed methodology. The provided examples of the existing operational practice in predicting seismic ground shaking are perfectly in line, or even anticipating, the guidelines and recommendations given in the Report of the International Commission on Earthquake Forecasting (Jordan *et al*., 2011).

Acknowledgments. We are grateful to L. Romashkova for her fundamental contribution to the stability analysis of the intermediate-term middle-range earthquake predictions and related data. We acknowledge Giancarlo Neri and Mircea Radulian for their suggestions, which significantly contributed improving the text of the manuscript. This study has benefited from funding provided by the Italian Presidenza del Consiglio dei Ministri - Dipartimento della Protezione Civile (DPC), Project S3-2012. This paper does not necessarily represent DPC official opinion and policies. A. Gorshkov has been partially supported by RFBR, grant 13-05-91167.

REFERENCES

Aki K.; 1987: *Strong motion seismology*. In: Erdik M. and Toksöz M. (eds), NATO ASI Series, Series C: Math. and Phys. Sci., D. Reidel Publishing Company, Dordrecht, **204**, pp. 3-39.

Alekseevskaya M.A., Gabrielov A.M., Gvishiani A.D., Gelfand I.M. and Ranzman E.Y.; 1977: *Formal morphostructural zoning of mountain territories*. J. Geophys., **43**, 227-233.

Anonymous; 1983: *Guidelines for earthquake predictors*. Bull. Seismol. Soc. Am., **73**, 1955-1956.

Bhatia S.C., Chetty T.R.K., Filimonov M., Gorshkov A., Rantsman E. and Rao M.N.; 1992: *Identification of potential areas for the occurrence of strong earthquakes in Himalayan Arc Region*. Proc. Indian Acad. Sci. (Earth Planet. Sci), **101**, 369-385.

Bongard M.M.; 1967: *Problema uznavaniya (The recognition problem)*. Nauka, Moscow, Russia, (in Russian).

Bormann P.; 2011: *From earthquake prediction research to time-variable seismic hazard assessment applications*. Pure Appl. Geophys., **168**, 329-366, doi: 10.1007/s00024-010-0114-0

Bragato P.L., Sugan M., Augliera P., Massa M., Vuan A. and Saraò A.; 2011: *Moho reflection effects in the Po Plain (northern Italy) observed from instrumental and intensity data*. Bull. Seismol. Soc. Am., **101**, 2142-2152, doi: 10.1785/0120100257.

Brune J.N. and Whitney J.W.; 2000: *Precarious rocks and seismic shaking at Yucca mountain, Nevada*. In: Whitney J.W. and Keefer W.R. (eds), Geologic and Geophysical Characterization Studies of Yucca Mountain, Nevada, A Potential High-Level Radioactive-Waste Repository, U.S. Geological Survey, Digital Series DS-058, Chapter M, pp. 1-19.

Burger W., Sommerville P.G., Barker J.S., Herrmann R.B. and Helmberger D.V.; 1987: *The effect of crustal structure on strong ground motion attenuation relations in eastern North America*. Bull. Seismol. Soc. Am., **77**, 1274-1294.

Burrato P., Ciucci F. and Valensise G.; 2003: *An inventory of river anomalies in the Po Plain, northern Italy: evidence for active blind thrust faulting*. Ann. Geophys., **46**, 865-882.

Camassi R. and Stucchi M.; 1997: *NT4.1.1, un catalogo parametrico di terremoti di area italiana al di sopra della soglia del danno*. GNDT, Milano, Italy, 95 pp.

Caputo M., Keilis-Borok V., Oficerova E., Ranzman E., Rotwain I. and Solovjeff A.; 1980: *Pattern recognition of earthquake-prone areas in Italy.* Phys. Earth Planet. Int., **21**, 305-320.

Castiglioni G.B.; 1999: *Geomorphology of the Po Plain*. Geogr. Fis. Din. Quat. (Suppl.), **III**, 7-20.

Chunga K., Michetti A., Gorshkov A., Panza G.F., Soloviev A. and Martillo C.; 2010: *Identificacion de nudos sismogenicos capaces de generar potenciales terremotos de M>6 y M>6.5 en la Región costera y cadenas montanosas de los Andes Septentrionales del Ecuador.* Revista ESPOL-RTE, **23**, 61-89.

Cisternas A., Godefroy P., Gvishiani A., Gorshkov A., Kossobokov V., Lambert M., Rantsman E., Sallantin J., Saldano H., Soloviev A. and Weber C.; 1985: *A dual approach to recognition of earthquake prone-areas in the western Alps*. Ann. Geophys., **3**, 249-270.

Crippa B., Sabadini R., Chersich M., Barzaghi R. and Panza G.F.; 2008: *Coupling geophysical modelling and geodesy to unravel the physics of active faults.* In: 2nd Workshop on Use of Remote Sensing Techniques for Monitoring Volcanoes and Seismogenic Areas, USEReST'08, Napoli, Italy, pp. 6-10, doi: 10.1109/USEREST.2008.4740331.

Decanini L.D. and Mollaioli F.; 1998: *Formulation of elastic earthquake input energy spectra*. Earthquake Eng. Struct. Dyn., **27**, 1503-1522.

Fäh D. and Panza G.F.; 1994: *Realistic modeling of observed seismic motion in complex sedimentary basins*. Ann. Geofis., **37**, 1771-1797.

Gabrielov A., Keilis-Borok V. and Jackson D.; 1996: *Geometric incompatibility in a fault system*. Proc. Natl. Acad. Sci. U.S.A., **93**, 3838-3842.

Gasperini P., Lolli B. and Vannucci G.; 2013: *Empirical calibration of local magnitude data sets versus moment magnitude in Italy.* Bull. Seismol. Soc. Am., **103**, 2227-2246, doi: 10.1785/0120120356.

Gelfand I.M., Guberman Sh.A., Izvekova M., Keilis-Borok V.I. and Rantsman E.Ya.; 1972: *Criteria of high seismicity determined by pattern recognition*. Tectonophys., **13**, 415-422.

Gelfand I.M., Guberman Sh.A., Zhidkov M.P., Keilis-Borok V.I., Ranzman E.Ya. and Rotwain I.M.; 1974a: *Recognition of earthquake-prone areas. II. Four regions in Asia Minor and South-East Europe*. In: Keilis-Borok V.I. (ed), Computational seismology, Computerized analysis of digital seismic data, vol. 7, Nauka, Moscow, Russia, pp. 3-40.

Gelfand I.M., Guberman Sh.A., Zhidkov M.P., Keilis-Borok V.I., Ranzman E.Ya. and Rotwain I.M.; 1974b: *Recognition of earthquake-prone areas. III. The case when the boundaries of disjunctive nodes are not known*. In: Keilis-Borok V.I. (ed), Computational seismology, Computerized analysis of digital seismic data, vol. 7, Nauka, Moscow, Russia, pp. 41-64.

Gelfand I.M., Guberman Sh.A., Keilis-Borok V.I., Knopoff L., Press F., Ranzman I.Ya., Rotwain I.M. and Sadovsky A.M.; 1976: *Pattern recognition applied to earthquake epicenters in California*. Phys. Earth Planet. Inter., **11**, 227-283.

Geller R.J.; 2011: *Shake-up time for Japanese seismology*. Nature, **472**, 407-409.

Giardini D., Grünthal G., Shedlock K.M. and Zhang P.; 1999: *The GSHAP Global Seismic Hazard Map*. Ann. Geofis., **42,** 1225-1228.

Girdler R.W. and McConnell D.A.; 1994: *The 1990 to 1991 Sudan earthquake sequence and the extent of the East African Rift System*. Sci., **264**, 67-70.

Gorshkov A. and Gaudemer Y.; 2012: *Identification of seismogenic nodes in an area of low seismicity (case of the Massif Central, France)*. In: Abstracts 33rd General Assembly of the European Seismological Commission, Moscow, Russia, p. 380

Gorshkov A., Zhidkov M., Rantsman E. and Tumarkin A.; 1991: *Morphostructures of the Lesser Caucaus and places of earthquakes, M≥5.5*. Izv. Acad. Sci. SSSR, Phys Earth., **6**, 30-38.

Gorshkov A., Kuznetsov I., Panza G.F. and Soloviev A.; 2000: *Identification of future earthquake sources in the Carpatho-Balkan orogenic belt using morphostuctural criteria*. Pure Appl. Geophys., **157**, 79-95.

Gorshkov A.I., Panza G.F., Soloviev A.A. and Aoudia A.; 2002: *Morphostructural zonation and preliminary recognition of seismogenic nodes around the Adria margin in peninsular Italy and Sicily.* J. Seismol. Earthquake Eng., **4,** 1-24.

Gorshkov A., Kossobokov V. and Soloviev A.; 2003: *Recognition of earthquake-prone areas*. In: Keilis-Borok V. and Soloviev A. (eds), Nonlinear Dynamics of the Lithosphere and Earthquake Prediction, Springer, Heidelberg, Germany, pp. 239-310.

Gorshkov A.I., Panza G.F., Soloviev A.A. and Aoudia A.; 2004: *Identification of seismogenic nodes in the Alps and Dinarides*. Boll. Soc. Geol. Ital., **123**, 3-18.

Gorshkov A.I., Kossobokov V.G., Rantsman E.Ya. and Soloviev A.A.; 2005: *Recognition of earthquake-prone areas: validity of results obtained from 1972 to 2000*. Comput. Seismol. Geodyn., **7**, 37-44.

Gorshkov A., Mokhtari M. and Piotrovskaya E.; 2009a: *The Alborz region: identification of seismogenic nodes with morphostructural zoning and pattern recognition*. J. Seismol. Earthquake Eng., **1**, 1-15.

Gorshkov A.I., Panza G.F., Soloviev A.A., Aoudia A. and Peresan A.; 2009b: *Delineation of the geometry of nodes in the Alps-Dinarides hinge zone and recognition of seismogenic nodes*. Terra Nova, **21**, 257-264.

Gorshkov A.I., Soloviev A.A., Jiménez M.J., García-Fernández M. and Panza G.F.; 2010: *Recognition of earthquake-prone areas (M≥5.0) in the Iberian Peninsula*. Rendiconti Lincei - Scienze Fisiche e Naturali, **21**, 131-162, doi: 10.1007/s12210-010-0075-3.

Gruppo di Lavoro MPS; 2004: *Redazione della mappa di pericolosità sismica prevista dall'Ordinanza PCM 3274 del 20 marzo 2003. Rapporto conclusivo per il Dipartimento della Protezione Civile*. INGV, Milano-Roma, 65 pp. + 5 appendici.

Gulkan P.; 2013: *A dispassionate view of seismic-hazard assessment*. Seismol. Res. Lett., **84**, 413-416, doi: 10.1785/0220130005.

Gusev A.A.; 1983: *Descriptive statistical model of earthquake source radiation and its application to an estimation of short period strong motion*. Geophys. J. R. Astron. Soc., **74**, 787-800.

Gvishiani A.D. and Soloviev A.A.; 1981: *Association of the epicenters of strong earthquakes with the intersection of morphostructural lines in South America*. Comput. Seismol., **13**, 42-47.

Gvishiani A.D. and Soloviev A.A.; 1984: *Recognition of places on the Pacific coast of the South America where strong earthquakes may occur.* Earthquake Predict. Res., **2**, 237-243.

Gvishiani A.D., Zhidkov M.P. and Soloviev A.A.; 1984: *On application of the criteria of high seismicity of Andean mountain belt to Kamchatka*. Izv. Akad. Nauk SSSR, Fiz. Zemli, **1**, 20-33.

Gvishiani A., Gorshkov A., Kossobokov V., Cisternas A., Philip H. and Weber C.; 1987: *Identification of seismically dangerous zones in the Pyrenees*. Ann. Geophys., **5**, 681-690.

Gvishiani A.D., Gorshkov A.I., Ranzman E.Ya., Cisternas A. and Soloviev A.A.; 1988: *Prognozirovanie mest zemletryasenii v regionakh umerennoi seismichnosti (Forecasting the earthquake locations in the regions of moderate seismic activity)*. Nauka, Moscow, Russia, 187 pp.

Handy M.R., Schmid S.M., Bousque R., Kissling E. and Bernoulli D.; 2010: *Reconciling plate-tectonic reconstructions of Alpine Tethys with the geological-geophysical record of spreading and subduction in the Alps*. Earth Sci. Rev., **102**, 121-158.

Healy J.H., Kossobokov V.G. and Dewey J.W.; 1992: *A test to evaluate the earthquake prediction algorithm, M8*. U.S. Geol. Surv., Open-File Report 92-401, 23 pp. + 6 Appendices.

Hobbs W.N.; 1904: *Lineaments of the Atlantic border region*. Bull. Geol. Soc. Am., **15**, 483-506.

Hudnut K.W., Seeber L. and Pacheo J.; 1989: *Cross-fault triggering in the November 1987 Superstition Hills earthquake sequence, southern California*. Geophys. Res. Lett., **16**, 199-202.

ISIDe Working Group; 2015: *ISIDe Italian Seismological Instrumental and parametric Database*. http://iside.rm.ingv.it/iside/standard/index.jsp.

Jordan T., Chen Y., Gasparini P., Madariaga R., Main I., Marzocchi W., Papadopoulos G., Sobolev G., Yamaoka K. and Zschau J.; 2011: *ICEF Report, operational earthquake forecasting: state of knowledge and guidelines for utilization*. Ann. Geophys., **54**, 315-391.

Kanamori H.; 2003: *Earthquake prediction: an overview.* In: Lee W.H.K., Kanamori H., Jennings J.C. and Kisslinger C. (eds), International Handbook of Earthquake and Engineering Seismology, Academic Press, San Diego, CA, USA, Part B, pp. 1205-1216.

Kantorovich L.V. and Keilis-Borok V.I.; 1991: *Earthquake prediction and decision-making: social, economic and civil protection aspects*. In: Proc. International Conference on Earthquake Prediction, State-of-the-Art, Strasbourg, France, pp. 586-593.

Keilis-Borok V.I. and Kossobokov V.G.; 1990: *Preliminary activation of seismic flow: algorithm M8*. Phys. Earth Planet. Inter., **61**, 73-83.

Keilis-Borok V.I. and Rotwain I.; 1990: *Diagnosis of time of increased probability of strong earthquakes in different regions of the world: algorithm CN*. Phys. Earth Planet. Inter.**, 61**, 57-72.

Keilis-Borok V.I. and Soloviev A.A. (eds); 2003; *Non-linear dynamics of the lithosphere and earthquake prediction*. Springer, Heidelberg, Germany, 337 pp.

King G.; 1986: *Speculations on the geometry of the initiation a termination processes of earthquake rupture and its relation to morphology and geological structure*. Pure Appl. Geophys., **124**, 567-583.

Kossobokov V.; 2005: *Regional earthquake likelihood models: a realm on shaky grounds?* Am. Geophys. Union, **86**, Abstr. S41D-08.

Kossobokov V.; 2008: *Testing earthquake forecast/prediction methods: "Real-time forecasts of tomorrow's earthquakes in California"*. Geophys. Res. Abstr., **10**, EGU2008-A-07826.

Kossobokov V.; 2009: *Testing earthquake forecast/prediction methods: "Real-time forecasts of tomorrow's earthquakes in California"*. In: Some Problems of Geodynamics, KRASAND, Comput. Seismol., 39, Moscow, Russia, pp. 321-337, (in Russian).

Kossobokov V.; 2012: *Earthquake prediction: 20 years of global experiment*. Nat. Hazards, **69,** 1155-1177, doi: 10.1007/s11069-012-0198-1.

Kossobokov V. and Shebalin P.; 2003: *Earthquake Prediction*. In: Keilis-Borok V.I. and Soloviev A.A. (eds), Non-linear dynamics of the lithosphere and earthquake prediction, Springer, Heidelberg, Germany, pp. 141-207.

Kossobokov V.G., Romashkova L.L., Keilis-Borok V.I. and Healy J.H.; 1999: *Testing earthquake prediction algorithms: statistically significant advance prediction of the largest earthquakes in the Circum-Pacific, 1992-1997*. Phys. Earth Planet. Inter., **111**, 187-196.

Kossobokov V.G., Romashkova L.L., Panza G.F. and Peresan A.; 2002: *Stabilizing intermediate-term medium-range earthquake predictions*. J. Seismol. Earthquake Eng., **8**, 11-19.

Kossobokov V.G., Peresan A. and Panza G.F.; 2015: *On operational earthquake forecast and prediction problems*. Seismol. Res. Letters, **82**, 287-290.

Livio F.A., Berlusconi A., Michetti A.M., Sileo G., Zerboni A., Trombino L., Cremaschi M., Mueller K., Vittori E., Carcano C. and Rogledi S.; 2009: *Active fault-related folding in the epicentral area of the December 25, 1222 (I0=IX MCS) Brescia earthquake (northern Italy): seismotectonic implications*. Tectonophys., **476**, 320-335.

Meletti C. and Valensise G.; 2004: *Zonazione sismogenetica ZS9 - App. 2 al Rapporto Conclusivo*. Gruppo di Lavoro MPS; 2004: Redazione della mappa di pericolosità sismica prevista dall'Ordinanza PCM 3274 del 20 marzo 2003. Rapporto conclusivo per il Dipartimento della Protezione Civile. INGV, Milano-Roma, 65 pp. + 5 appendici.

Michetti A.M., Giardina F., Livio F., Mueller K., Serva L., Sileo G., Vittori E., Devoti R., Riguzzi F., Carcano C., Rogledi S., Bonadeo L., Brunamonte F. and Fioraso G.; 2012: *Active compressional tectonics, Quaternary capable faults, and the seismic landscape of the Po Plain (N Italy)*. Ann. Geophys., **55**, 969-1001, doi: 10.4401/ag-5462.

Molchan G., Kronrod T. and Panza G.F.; 1997: *Multi-scale seismicity model for seismic risk*. Bull. Seismol. Soc. Am., **870**, 1220-1229.

Mridula, Sinhval A. and Wason H.R; 2013: *A review on pattern recognition techniques for seismic hazard analysis*. In: Proc. International Conference on Emerging Trends in Engineering and Technology, pp. 854-858, doi: 03.AETS.2013.3.4_1.

Nekrasova A., Kossobokov V., Peresan A. and Magrin A.; 2014: *The comparison of the NDSHA, PSHA seismic hazard maps and real seismicity for the Italian territory*. Nat. Hazards, **70**, 629-641, doi: 10.1007/s11069-013-0832-6.

Novikova O. and Gorshkov A.; 2013: *Recognition of earthquake prone areas (M≥6.0) in the Kopet Dagh region using the GIS technology*. J. Seismol. Earthquake Eng., **15**, 92-99.

Novikova O., Soloviev A. and Gorshkov A.; 2012: *Recognition of areas prone to large earthquakes in the Caspian-Black Sea region*. In: Abstracts 33rd General Assembly of the European Seismological Commission, Moscow, Russia, p. 334.

Panza G.F. and Suhadolc P.; 1989: *Realistic simulation and prediction of strong ground motion*. In: Carlomagno G.M. and Brebbia C.A. (eds), Computers and experiments in stress analysis, Springer-Verlag, Berlin, Germany, pp. 77-98.

Panza G.F., Peresan A. and Vaccari F.; 2009: *La previsione dei terremoti: stato dell'arte*. Geoitalia, **28**, 18-23 (in Italian).

Panza, G.F., Peresan A. and Zuccolo E.; 2010: *Climatic modulation of seismicity in the Alpine-Himalayan mountain range*. Terra Nova, **23**, 19-25, doi: 10.1111/j.1365-3121.2010.00976.x.

Panza G.F., Peresan A., Magrin A., Vaccari F., Sabadini R., Crippa B., Marotta A.M., Splendore R., Barzaghi R., Borghi A., Cannizzaro L., Amodio A. and Zoffoli S.; 2011: *The SISMA prototype system: integrating geophysical modeling and Earth observation for time-dependent seismic hazard assessment*. Nat. Hazards, **69**, 1179-1198, doi: 10.1007/s11069-011-9981-7.

Panza G.F., La Mura C., Peresan A., Romanelli F. and Vaccari F.; 2012: *Seismic hazard scenarios as preventive tools for a disaster resilient society*. Adv. Geophys., **53**, 93-165, doi: 10.1016/B978-0-12-380938-4.00003-3.

Panza G.F., Kossobokov V., Peresan A. and Nekrasova A.; 2014: *Why are the standard probabilistic methods of estimating seismic hazard and risks too often wrong?* In: Wyss M. (ed), Earthquake Hazard, Risk, and Disasters, Elsevier, London, UK, Chapter 12, pp. 309-357, doi: 10.1016/B978-0-12-394848-9.00012-2.

Paskaleva I., Dimova S., Panza G.F. and Vaccari F.; 2007: *An earthquake scenario for the microzonation of Sofia and the vulnerability of structures designed by use of the Eurocodes*. Soil. Dyn. Earthquake Eng., **27**, 1028-1041.

Peresan A. and Panza G.F.; 2002: *UCI2001: the updated catalog of Italy*. ICTP, Trieste, Italy, Internal report, IC/IR/2002/3.

Peresan A., Costa G. and Panza G.F.; 1999: *Seismotectonic model and CN earthquake prediction in Italy*. Pure Appl. Geophys., **154**, 281-306.

Peresan A., Panza G.F. and Costa G.; 2000: *CN algorithm and long lasting changes in reported magnitudes: the case of Italy*. Geophys. J. Int., **141**, 425-437.

Peresan A, Rotwain I., Zaliapin I. and Panza G.F.; 2002: *Stability of intermediate-term earthquake predictions with respect to random errors in magnitude: the case of central Italy*. Phys. Earth Planet. Inter., **130**, 117-127.

Peresan A., Kossobokov V., Romashkova L. and Panza G.F., 2005: *Intermediate-term middle-range earthquake predictions in Italy: a review*. Earth Sci. Rev., **69**, 97-132.

Peresan A., Zuccolo E., Vaccari F., Gorshkov A. and Panza G.F.; 2011: *Neo-deterministic seismic hazard and pattern recognition techniques: time dependent scenarios for North-Eastern Italy*. Pure Appl. Geophys., **168**, 583-607, doi: 10.1007/s00024-010-0166-1.

Peresan A., Magrin A., Vaccari F. and Panza G.F.; 2012: *Prospective testing of time-dependent neo-deterministic seismic hazard scenarios*. In: Atti 31th GNGTS, Potenza, Italy, pp. 429-433.

Rantsman E.Ya.; 1979: *Sites of earthquakes and morphostructures of Mountain Countries*. Nauka, Moscow, Russia, 172 pp., (in Russian).

Romashkova L. and Peresan A.; 2013: *Analysis of Italian earthquake catalogs in the context of intermediate-term prediction problem*. Acta Geophys., **61**, 583-610, doi: 10.2478/s11600-012-0085-x.

Romashkova L., Peresan A. and Nekrasova A.; 2009: *Analysis of earthquake catalogs for CSEP testing region Italy.* ICTP, Trieste, Italy, Internal report, IC/IR/2009/006.

Rotwain I.M. and Novikova O.; 1999: *Performance of the earthquake prediction algorithm CN in 22 regions of the world*. Phys. Earth Planet. Inter., **111**, 207-213.

Rovida A., Camassi R., Gasperini P. and Stucchi M. (eds); 2011: *CPTI11, the 2011 version of the Parametric Catalogue of Italian Earthquakes*. Milano, Bologna, http://emidius.mi.ingv.it/CPTI, doi: 10.6092/INGV.IT-CPTI11.

Soloviev A.A., Novikova O.V., Gorshkov A.I. and Piotrovskaya E.P.; 2013: *Recognition of potential sources of strong earthquakes in the Caucasus Region using GIS technologies*. Doklady Earth Sci., **450**, 658-660, doi: 10.1134/S1028334X13060159.

Soloviev A.A., Gvishiani A.D., Gorshkov A.I., Dobrovolsky M.N. and Novikova O.V.; 2014: *Recognition of earthquake-prone areas: methodology and analysis of the results*. Izv. Phys. Solid Earth, **50**, 151-168, doi: 10.1134/S1069351314020116.

Stein S., Geller R. and Liu M.; 2012: *Why earthquake hazard maps often fail and what to do about it*. Tectonophys., **562-563**, 1-25.

Stein S., Geller R. and Liu M.; 2013: *Reply to comment by Arthur Frankel on "Why earthquake hazard maps often fail and what to do about it"*. Tectonophys., **592**, 207-209.

Talwani P.; 1988: *The intersection model for intraplate earthquakes*. *Seismol*. *Res*. *Lett*., **59**, 305-310.

Talwani P.; 1999: *Fault geometry and earthquakes in continental interiors*. *Tectonophys*., **305**, 371-379.

Toscani G., Burrato P., Di Bucci D., Seno S. and Valensise G.; 2009: *Plio-Quaternary tectonic evolution of the northern Apennines thrust fronts (Bologna-Ferrara section, Italy): seismotectonic implications*. Boll. Soc. Geol. It., **128**, 605-613, doi: 10.3301/IJG.2009.128.2.605).

Tuyen N.H., Gorshkov A.I. and Lu N.T.; 2012: *Recognition of earthquake-prone areas (M≥5.0) applied for North Vietnam and adjacency.* J. Sci. Earth, **34**, 251-265.

Uang C.M. and Bertero V.V.; 1990: *Evaluation of seismic energy in structures*. Earthquake Eng. Struct. Dyn., **19**, 77-90.

Vaccari F., Peresan A., Zuccolo E., Romanelli F., Marson C., Fiorotto V. and Panza G.F.; 2009: *Neo-deterministic seismic hazard scenarios: application to the engineering analysis of historical buildings*. In: Mazzolani (ed), Proc. PROHITECH 2009, Protection of Historical Buildings, Taylor & Francis Group, London, UK, pp. 1559-1564.

Vorobieva I. and Panza G.F.; 1993: *Prediction of the occurrence of related strong earthquakes in Italy.* Pure Appl. Geophys., **141,** 25-41.

Wells D.L. and Coppersmith K.J.; 1994: *New empirical relationships among magnitude, rupture length, rupture width, and surface displacement*. Bull. Seismol. Soc. Am., **84**, 974-1002.

Wyss M., Nekrasova A. and Kossobokov V.; 2012: *Errors in expected human losses due to incorrect seismic hazard estimates*. Nat. Hazards, **62**, 927-935, doi: 10.1007/s11069-012-0125-5.

Zuccolo E., Vaccari F., Peresan A. and Panza G.F.; 2011: *Neo-deterministic (NDSHA) and probabilistic seismic hazard (PSHA) assessments: a comparison over the Italian territory.* Pure Appl. Geophys., **168**, 69-83, doi: 10.1007/s00024-010-0151-8.

Corresponding author: Antonella Peresan
Department of Mathematics and Geosciences, University of Trieste
Via Edoardo Weiss 4, 34127 Trieste, Italy
Phone: +39 040 5582129; fax: +39 040 5582111; e-mail: aperesan@units.it